Reactive Oxygen Species mediated regulation of autophagy in Skeletal Muscles.

Mashrur Rahman

Faculty of Medicine

Division of Experimental Medicine

McGill University, Montreal, QC

August, 2013

A thesis submitted to McGill University in partial fulfillment of the requirements of the degree of Master of Science

TABLE OF CONTENTS

ABSTRACT

Skeletal muscles comprise of approximately 50% of the human body mass and are critical organs for enabling locomotion and exerting metabolic control. Autophagy, a lysosome-dependant catabolic process involved in the degradation of long-lived proteins and organelles, is an important process responsible for maintaining muscle homeostasis. Reactive Oxygen Species (ROS) has been shown to induce autophagy in many different cell types. In this study, we evaluate the effects of physiological levels of mitochondrial-derived reactive oxygen species (ROS) on skeletal muscle autophagy.

In differentiated C2C12 myotubes, basal level autophagy and autophagy triggered by 1.5 to 4 hr of acute nutrient deprivation, inhibition of mTORC1, or leucine deprivation were quantified using a long-lived protein degradation assay (index of proteolysis), LC3B autophagic flux, and mRNA expressions of autophagy-related genes. Pre-incubation with antioxidants tempol (SOD mimetic) or N-acetyl cysteine (NAC) significantly attenuates rates of proteolysis and LC3B flux and blocks increases in acute and nutrient deprivation-, rapamycin treatment- and leucine deprivation-triggered autophagy. Similar results were obtained with mitochondira-specific antioxidants mito-tempol and SS31. MitoSOX^{TM} Red fluorescence measurements confirm that mitochondrial ROS levels increase substantially in response to acute nutrient deprivation and rapamycin treatment and that tempol and mito-tempol attenuates this response. Antioxidants decrease AMPK phosphorylation by 40% and significantly augment AKT phosphorylation, but exert no effects on mTORC1-dependant ULK1 phosphorylation on Ser^{555}. Treatment of mice with NAC significantly attenuated basal LC3B autophagic flux in the diaphragm, confirming that endogenous ROS promotes *in vivo* muscle autophagy.

We report for the first time that mitochondrial-derived ROS promote skeletal muscle autophagy and that this effect is mediated in part through AKT inhibition and autophagy initiation via AMPK activation.

RÉSUMÉ

Les muscles squelettiques constituent environ 50% de la masse du corps humain et représente un organe essentiel permettant la locomotion et le contrôle métabolique. L'autophagie, un processus catabolique lysosome-dépendant, est impliquée dans la dégradation des protéines et des organites à long terme. Elle représente un processus important pour le maintien de l'homéostasie du muscle. Par ailleurs, il a été montré que les radicaux libres (ROS) principalement générés par les mitochondries, induisent l'autophagie dans de nombreux types cellulaires. Dans cette étude, nous voulons évaluer des radicaux libres mitochondriaux (ROS) à un niveau physiologique sur l'autophagie dans le muscle squelettique

Dans les myotubes différenciés C2C12, le niveau basal de l'autophagie et son activation (déclenchées par 1,5 à 4 h de carence aigüe en nutriments, par l'inhibition de mTORC1, ou encore par la privation en leucine) ont été quantifiés à l'aide d'un test de longue durée de dégradation des protéines (indice de protéolyse), par le flux d'autophagie LC3B, ou par les l'ARNm des gènes liés à l'autophagie. La pré-incubation avec des antioxydants de type tempol (SOD mimétique) ou N-acétylcystéine (NAC) atténue considérablement les niveaux de protéolyse, de flux de LC3B et bloque l'activation de l'autophagie secondaire à la carence en nutriments –traitement par rapamycine- ou la carence en leucine. Des résultats similaires ont été obtenus avec es antioxydants spécifiques de la mitochondrie mito-tempol et SS31. Des mesures de fluorescence rouge MitoSOX^{TM} confirment que le niveau de radicaux libres mitochondriaux augmentent considérablement en réponse à une carence en nutriments aiguë ou au traitement par rapamycine et que le tempol et mito-tempol atténue cette réponse. Les antioxydants entraîne une diminution de 40% de la phosphorylation de l'AMPK et augmente significativement la phosphorylation de l'AKT, mais sans exercer aucun effet sur mTORC1 qui est dépendant de la

phosphorylation sur Ser555 ULK1. Le traitement des souris avec NAC atténue significativement le flux autophagique basal de LC3B dans le diaphragme, ce qui confirme que les ROS endogènes favorise l'autophagie musculaire in vivo.

Nous rapportons pour la première fois que les ROS mitochondriaux sont responsable de l’activation de l’autophagie dans le muscle squelettique et que cet effet est médié en partie par l'inhibition de AKT et de l'initiation de l'autophagie par activation de l'AMPK.

AKNOWLEDGEMENTS

First of all, I would like to express my deepest gratitude to my research supervisor, Dr.Sabah N.A.Hussain for giving me the opportunity at a difficult period in my life to join his research group. I have been privileged to have been mentored by such an excellent scientist and human being. Over the last two years, the lessons I have learnt from him regarding every walks of life will serve me well into the future. Moreover, I am glad he is such as soccer fanatic as I am! I would also like to express my sincere appreciation and thankfulness for each and every member of the Critical Care Division Research Laboratory namely Dominique Mayaki, Angela Stamiris, Flora Golyardi, Raquel Echavarria, Marija Vujovic, Hodan Ismail and Kwan-bo Joung. I would like to thank Christine Mutter and Irene Prager for their kind assistance whenever I needed help with administrative issues. I wish to thank all the members of my thesis committee, Dr.Suhad Ali, Dr. Russ Hepple, Dr. Thomas Jagoe and especially Dr. Arnold Kristoff for providing special insight and guidance with my research project. I would like to acknowledge Dr. Peter Schiller and Dr. Jacques Genest for providing me with the useful materials for conducting experiments.

To Mahroo Mafarrahi I owe you so much for being such as kind mentor and friend. I thank you for teaching me most of the technical and research skills that I now possess, troubleshooting with me and most importantly, listening to me when I had problems be it research oriented or not.

To Bernard Nkengfac, thank you for being such a good mentor, friend and providing a jovial atmosphere to work in. All those days we spent doing late night experiments and talking about "El Classico" will never be forgotten.

To Mary (MJ)- thank you for becoming my dear sister in every possible way. It will be a relationship that I will cherish forever.

To Sharon Harel, I owe special thanks to you for providing such important insight into my research work on one hand and my spiritual life in the other.

I would also like to express my special gratitude to all the summer and exchange students I had the fortune to come across during my two years. I would also like to show my appreciation for Dr. Hugh Bennett and the ExMed team of Dominique and Marilyn. Without their assistance I would have been truly lost. Moreover, I am indebted to my mother, father and brother whose constant source of encouragement was a cornerstone for my accomplishment. Finally and most importantly, I would like to thank God, the Almighty for allowing me to achieve this deed.

LIST OF ABBREVIATIONS:

AKTi: Akt inhibitor (triciribine)

AMPK: AMP-activated protein kinase

Ant.A: Antimycin A

Baf A1: Bafilomycin A1

Bnip3: BCl2/adenovirus E1B 19kD-interacting protein 3

DM: Differentiation medium

DMEM: Dulbecco's Modified Eagle Medium

DMSO: Dimethyl sulfoxide

EBSS: Earle's Balanced Salt Solution

EDTA: Ethylenediaminetetraacetic acid

FBS: Fetal bovine serum

FOXO3A: Forkhead Box 03

Gabarapl1: Gamma-aminobutyric acid receptor-associated protein-like 1

HBSS: Hank's Balanced Salt Solution

i.p. Intraperitoneal

LC3B: Microtubule-associated protein 1 light chain 3 beta

Leu(-): Leucine deprivation

Mitotempol: (2-(2,2,6,6-Tetramethylpiperidin-1-oxyl-4-ylamino)-2-oxoethyl)triphenylphosphonium chloride.monohydrate

mTORC1: Mammalian target of rapamycin complex I

NAC: N-Acetyl cysteine

PBS: Phosphate buffered saline

PMSF: Phenylmethanes sulfonylfluoride

Rapa: Rapamycin

RPS6KB1: Ribosomal protein S6 kinase beta 1

ROS: Reactive oxygen species

SDS: Sodium dodecyl sulfate

SOD: Superoxide Dismutase

SQSTM1: Sequestome 1

Tempol: Hydroxy-2,2,6,6-tetramethylpiperidinyloxy

ULK1: Unc-51-like kinase 1

SECTION 1: INTRODUCTION

Skeletal muscles comprise of 50% of the human body mass and are critical organs for enabling locomotion and exerting metabolic control. In order to allow movement, highly structured muscle cells undergo contractions at regular intervals that require energy in the form of ATP to be produced in the mitochondria (175). This process, among other things, leads to the production of Reactive Oxygen Species (ROS). In muscles, relatively low physiological levels of ROS play important roles as signalling molecules in a wide range of physiological and pathophysiological responses (125). However, production of excessive amount of ROS in muscles can be exacerbated as a consequence of certain physiological stresses such as starvation, hypoxia, disuse and denervation leading to a condition known as oxidative stress. Oxidative stress has deleterious effects on many cellular components and can mechanically and metabolically damage muscle proteins and organelles (4; 27; 60). Therefore, muscle cells require an efficient system for removing and eliminating unfolded and toxic proteins as well as abnormal and dysfunctional organelles. The autophagy-lysosomal pathway serves this purpose in muscles by generating double-membrane vesicles that engulf portion of cytoplasm, organelles, glycogen, protein aggregates which are then fused with lysosomes for degradation (141). Proper regulation of the autophagic flux is fundamental for the homeostasis of skeletal muscles during physiological situations and in response to stress because defective or excessive autophagy is harmful for muscle health and has a pathogenic role in several forms of muscle disease (142). However, the role of physiological levels of mitochondrial derived ROS in inducing autophagy in skeletal muscles has not been properly elucidated. This thesis aims to investigate the effects of physiological levels of ROS on skeletal muscle autophagy using *in vitro* and *in vivo* models.

SECTION 2: LITERATURE REVIEW

2.1.1 Organization of Skeletal Muscles

Muscles are one of the most abundant soft tissues that are evolutionarily conserved across the animal kingdom (107). They are comprised of contractile proteins that slide past one another producing a contraction that changes both the length and shape of the cell. This produces the force that enables motion. Internally, this allows the flow of substance as well as movement of organs and externally, organisms can perform locomotion. In mammals, muscles are of 3 types. Firstly, smooth muscles are involuntary non-striated muscles lining blood vessels and alimentary canal regulating the passage of substances such as blood in the lumen of the space they occupy. Secondly, cardiac muscles are involuntary striated muscles forming the foundation of the heart and specifically the myocardium (62). Coordinated contractions and relaxations of cardiac muscles helps propel blood through the circulatory system of the body.

Skeletal muscles are the third type of muscles found in mammals and are the principle agents of locomotion for mammalian organisms. Skeletal muscles are attached to bones via tendons and upon contraction, enable gross movement. Individual progenitor muscle cells fuse and form long cylindrical multinucleated cells called myofibers. The cytosol of myofibers is highly organized, with contractile proteins assembled into repetitive structures called sarcomeres. Within each sarcomere are the myofibrillar proteins myosin (thick filament) and actin (thin filament). Interaction between these two myofibrillar proteins allows muscles to contract. Precise and coordinated movements are performed by these skeletal muscles due to this structural organization (141).

The nuclei are located at the edge of the myofibers, whereas the various organelles such as mitochondria and sarcoplasmic reticulum are embedded among the myofibrils. A proper organization and function of mitochondria and sarcoplasmic reticulum is fundamental for adequate supply of energy in the form of ATP and a correct release of calcium required for muscular contraction (65).

In the presence of ATP, the myosin head binds to actin and pulls the thin filament along the thick filament, allowing the sarcomere to shorten. As long as calcium ions (Ca^{2+}) and ATP are present, the myosin heads will attach to the actin molecule, pull the actin, release, and reattach. This process is known as cross-bridge cycling (175). The speed at which cross-bridge cycling can occur is limited predominantly by the rate that the ATPase of the myosin head can hydrolyze ATP.

Skeletal muscles are categorized based on the rate of myosin ATPase activity and the degree of oxidative phosphorylation these fibers undergo. Type I fibers are slow oxidative fibers and appear red. These fibers have many mitochondria, blood vessels and hydrolyze ATP at a slow rate. They are resistant to fatigue and are found in postural muscles (151). Type IIa fibers are fast oxidative fibers and have many mitochondria as well as the ability to hydrolyze ATP at a rapid rate. These fibers are resistant to fatigue, but not as much as the slow oxidative fibers. Type IIx fibers are fast glycolytic with few mitochondria, but with an ability to hydrolyze ATP extremely quickly. Type IIb fibers that are absent in humans but present in rodents are even more glycolytic in nature with a very high ATP hydrolysis rate. Mammalian skeletal muscles are heterogeneous in nature, with individual muscles being a mixture of these 3 types of muscle fibers and their proportions varying depending on the mammalian species in question as well as the position and function of the particular skeletal muscle (149).

2.1.2 Skeletal Muscle Atrophy

Muscle atrophy involves the shrinkage of myofibers due to a net loss of proteins, organelles and cytoplasm. Skeletal muscles comprise of approximately 50% of the human body mass and serve as the major reservoir of proteins in the body. Muscle proteins can be mobilized into free amino acids under disuse conditions (e.g. immobilization), in starvation and in many pathogenic states such as diabetes, cancer cachexia, sepsis, AIDS, burn injury, renal failure, trauma etc. This adaptation is highly beneficial under transient condition whereby free amino acids are made available for protein synthesis in obligatory-working organs like heart, lungs and the brain. However, sustained catabolic conditions leads to muscle wasting and can be extremely detrimental, especially when ventilatory muscles undergo atrophy (32). Moreover, muscle wasting is negatively associated with the ability of the individual to recover from stress or pathologies (33).

Skeletal muscle atrophy is mainly regulated by three distinct pathways; the calpain system which is comprised of Ca2+-sensitive proteases responsible for degradation of myofilaments into smaller peptides; the ubiquitin-proteasomal system which degrades myfilament peptides into individual amino acids; and the autophagy-lysosomal pathway (ALP) which is responsible for removal of long-lived cytoplasmic proteins and organelles such as mitochondria.

The calpain system cleaves the enormous myofibrillar proteins into smaller peptides. It comprises of a family Ca^{2+} dependant cysteine proteases that can modulate their substrates structure and function through limited proteolytic activity. The first tissue specific calpain subsequently called CAPN3 (p94) was discovered in skeletal muscles (159). It is responsible for

cleaving the connectin/titin protein which is an elastic filamentous muscle protein of approximately 30,000 kDa forming an essential part of the myofibrillar structure and playing a critical role for muscular contraction. Moreover, calpains have been shown to induce muscle atrophy in response to sepsis by increased expression of calpain 1, 2 and 3 mRNA (156). More recently Tidball et al. showed that by overexpressing a transgene of the endogenous inhibitor of calpains known as calpastatin, there was a 30% attenuation of the reduction in muscle fiber cross-sectional area compared with wild-type littermates (165). Recent evidence supports the notion that although they may not be important for bulk protein degradation, calpains may regulate the early rate-limiting steps involved in myofibrillar protein degradation (64). Since the ubiquitin-proteosome system cannot readily degrade intact large myofibrils, the calpain system takes over for this particular purpose (158).

Nevertheless, the bulk proteolysis in muscles is carried out by the ubiqiutin- proteosome system. Degradation of proteins via this multi-step pathway requires ATP hydrolysis, the protein co-factor ubiquitin and the 26S proteosome. The process of substrate ubiquitination involves the cooperative interaction of three classes of proteins termed E1 (ubiquitin activating), E2 (ubiquitin conjugating) and E3 (ubiquitin ligating) enzymes. The ubiquitin-activating enzyme (E1) utilizes ATP to create a highly reactive thiolester form of ubiquitin, and then transfers it to a ubiquitin-carrier protein (E2). The subsequent transfer of the activated ubiquitin to the substrate requires a ubiquitin-protein ligase (E3). The E3 enzyme confers specificity to the target protein. It binds the protein substrate and also the E2 carrying the activated ubiquitin, and transfers the activated ubiquitin from the E2 to the substrate. This is the rate-limiting step of the ubiquitination process. When a chain containing four or more ubiquitin molecules has been formed on the protein it is then usually degraded rapidly by the proteasome to yield small peptides The

targeted proteins are then digested within the central core of the 26S proteosome, which requires ATP for the degradation of proteins (45).

Only a few E3 enzymes have been found to regulate atrophy process and be transcriptionally induced in atrophying skeletal muscles. The first to be identified were Atrogin-1/MAFbx and MuRF1 (15; 46). Atrogin-1/MAFbx and MuRF1 knockout mice are resistant to muscle atrophy induced by denervation (15). MuRF1 knockout mice are also resistant to dexamethasone-induced muscle atrophy while, knockdown of atrogin-1 spares muscle mass in fasted animals (29). Thus far, MuRF1 ubiquitinates several muscle structural proteins, including troponin I (71), myosin heavy chains (25), actin (124), myosin binding protein C and myosin light chains 1 and 2 (26). Atrogin-1 promotes degradation of MyoD, a key muscle transcription factor, and of eIF3-f, an important activator of protein synthesis (166). Other E3 ligases important for muscle atrophy that were subsequently identified are Nedd4 and Mul1. Nedd4 is a HECT domain ubiquitin ligase and confers partial protection from denervation induced muscle atrophy (115). Mul 1, a mitochondrial specific ubiquitin ligase, has been shown to be involved in the removal of damaged mitochondria in skeletal muscle in response to muscle-wasting stimuli such as fasting (95).

Counteracting the ubiquitination process are de-ubiquitining enzymes (DUBs) among which ubiquitin-specific proteases (USPs) form the largest group. Little is known about the contribution of deubiquitination in relation to muscle atrophy, except for the fact that two USPs (USP14 and USP19) have been shown to be upregulated in atrophying muscles (28). Knock down of USP19 decreases protein degradation and dexamethasone induced loss of myosin heavy chain (162) implicating USPs could be generally important for the turnover process of making a pool of free ubiquitin available.

2.2 Autophagy

The third mechanism of regulation in skeletal muscle atrophy is the autophagy-lysosomal pathway. In brief, autophagy is a ubiquitous process in eukaryotic cells that results in the breakdown of cytoplasm in response to stress conditions which allows the cell to adapt to environmental and/or developmental changes. This process involves the invagination of cytosolic contents such as protein aggregates, damaged organelles and nutrient reserves by double-membraned vesicles which are subsequently fused with acidified lysosomes. Lysosomes were discovered by the late Dr.Christian de Duve in 1955 (31) later in 1963 he introduced the term 'autophagy' to the scientific world. In the late 1990s, with better technologies in molecular biology being made available, research in the field of autophagy exploded.

So far, 3 forms of autophagy have been identified: macroautophagy, microautophagy and chaperone-mediated autophagy. Macroautophagy stars with the de novo formation of cup-shaped isolation of double-membrane that engulfs a portion of the cytoplasm (80). Microautophagy involves the engulfment of cytoplasm instantly at the lysosomal membrane by invagination, protrusion and separation (106). Chaperone-mediated autophagy is the process of direct transport of unfolded proteins via the lysosomal chaperonin hsc70 and LAMP2A (10; 70).

This process is well conserved from yeast to mammals, and many of the autophagy-related (Atg) genes that are involved were originally identified in yeast (110). Macroautophagy, being the most prevalent, is the subject of this study and will be henceforth referred to as "autophagy". The process of autophagy can be divided into several key stages: initiation, elongation, maturation and fusion with the lysosomes.

2.2.1 Stages of autophagy

The initiation process involves the formation of two macromolecular complexes: a complex of ULK1-Atg13-FIP200 and a complex of class III PI-3 kinase (PI3KC3) with Beclin-1 and p150.

In the first complex, Atg13 binds ULK1 and mediates their interaction with FIP200 (44). Under nutrient deprivation conditions, Atg13 and ULK1/2 are dephosphorylated (153). This activates Ulk1 to induce autophagosome formation by phosphorylating and activating FIP200 (58). FIP200 then translocates to the pre-autophagosomal membrane after starvation, and induces autophagy (67). Although this complex is essential for autophagy, the exact mechanism by which this complex triggers the pre-autophagosomal membrane formation is unknown.

The formation of new autophagosomes also requires the activity of the class III phosphatidylinositol 3-kinase (PI3K), Vps34. Vps34 is part of the autophagy-regulating macromolecular complex (class III PI3K complex) consisting of Beclin 1/Atg6, Atg14/barkor, and p150/Vps15 (63; 74). Phosphatidylinositol-3-phosphate (PI-3-P), the product of Vps34 activity, plays an essential role in the early stages of the autophagy pathway as evident by the colocalization of early autophagosome markers in PI-3-P-enriched structures that were formed upon starvation (5). Vps34 activity is enhanced upon its interaction with Beclin, an essential adaptor protein required for autophagy (42). Beclin has both autophagy promoting binding partners such as Ambra-1 (40), UVRAG (91) as well as autophagy inhibiting partners such as Bcl-2 or Bcl-X_L (121) and serves as an important node for initiating autophagy.

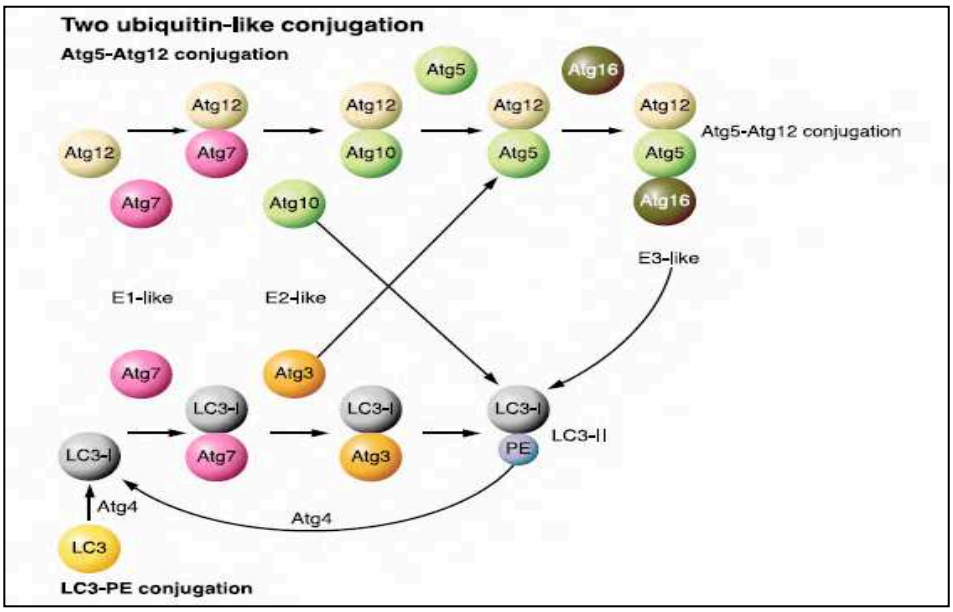

Diagram 1: Two ubiuitin-like conjugation system

The elongation process involves two ubiquitin like conjugation reactions (see diagram 1). Atg7, serving as an E-1 ubiquitin activating like enzyme is the common and essential mediator of these two conjugation reactions. Knock-out models of this gene exhibit complete impairment of autophagy (83). The Atg7 mediated reaction results in the formation of the Atg12-Atg5.Atg16L1 tetramer complex which dissociates upon assembly of the complete autophagosome (108). The other Atg7 mediated reaction results in the addition of a phosphatidylethanolamine (PE) moiety to LC3, GABARAP1 and GATE16 proteins. These proteins then persist on both the inner and outer membrane of the autophagosome until their fusion with lysosomes, when they are degraded. The relatively specific association of LC3-II with autophagosomes makes it an excellent marker for studying autophagy (81).

Another marker used in the measurement of autophagy is the protein SQSTM1, more commonly known as p62 which plays a unique role in the cross-talk between the ubiquitin-proteosomal and the autophagic pathways. p62, which itself is targeted to autophagosomes via its affinity for LC3, is a ubiquitin binding protein and helps some proteins and protein aggregates to

the autophagosome for degradation (78). Impairment of autophagy leads to accumulation of p62 (82).

The autophagosomes, along with their cargo, then migrate along microtubules to reach the lysosomes. Fusion with the lysosomes is mediated by proteins such as ESCRT, SNAREs, Rab7, and the class C Vps (3; 50; 136). UVRAG has been shown to be involved in the maturation step by recruiting fusion machinery on to the autophagosomes (92). In addition to fusion machinery, proper lysosomal function is also essential for fusion and degradation of autophagosomes to be successful. Inhibition of the lysosomal H^+- ATPase by chemicals like bafilomycin A1 inhibits the fusion of autophagosomes with lysosomes (179).

2.2.2 Autophagy and Skeletal Muscle

The predominant role of the ubiquitin-protesomal pathway in skeletal muscle atrophy was challenged by studies showing increased expression of the cathepsin lysosomal proteases in atrophying muscles from a variety of models of muscle wasting (35; 41; 163). In 2004, Mizushima et al. observed that a large number of GFP-positive vesicles in muscles of transgenic mice expressing GFP-LC3 in response to fasting, suggesting an increase in autophagy. Moreover, skeletal muscles were one of the tissues with the highest rate of autophagosome formation (109).

Importance of autophagy in skeletal muscle homeostasis was further established by using murine knock-out models of a few essential components of the autophagic machinery. Sandri et al. showed that Atg7-null mice are affected by muscle weakness and atrophy, and they display several signs of myopathy. Ablation of Atg7, the unique E1 enzyme of the autophagic machinery, causes disorganized sarcomeres and activation of the unfolded protein response,

which in turn triggers myofiber degeneration; this phenotype is associated with complete inhibition of autophagosome formation, leading to abnormal mitochondria, oxidative stress and accumulation of polyubiquitylated proteins (100). The same group showed that suppression of autophagy exacerbates fasting and denervation-induced atrophy in Atg7-null mice (101). A similar phenotype was observed in mice with muscle-specific ablation of Atg5, another crucial component of the autophagy machinery (127). Another recent mouse study revealed that nutrient-deprivation autophagy factor-1 (Naf-1), a Bcl-2-associated autophagy regulator, is required for the homeostatic maintenance of skeletal muscle. Naf1-null mice display muscle weakness and markedly decreased strength, accompanied by increased autophagy, dysregulation of calcium homeostasis and enlarged mitochondria (22).

The crucial role of the autophagy-lysosome system in skeletal muscles is confirmed by the fact that alterations to this process contribute to the pathogenesis of several genetic muscle diseases. Autophagy has been shown to play a protective role against muscle weakness and wasting in Bethlem myopathy and Ullrich congenital muscular dystrophy, which are two inherited muscle disorders associated with collagen VI deficiency (11; 48). In certain other muscular dystrophies, such as merosin-deficient congenital muscular dystrophy type 1A (MDC1A) in which mice lack an extracellular matrix protein laminin-2, there is a general upregulation of autophagy-related genes and pharmacological inhibition of autophagy significantly improves their dystrophic phenotype (21). Accumulation of autophagosomes, as a result of mutations in genes coding for lysosomal dysfunction leads to a group of muscle disorders which include Pompe disease, Danon disease and X-linked myopathy with excessive autophagy (XMEA) (97; 128). Moreover, autophagy has been found to be modulated in skeletal muscles by a plethora of stimulus such as cancer (122), ageing (174; 177), fasting (98), caloric

restriction (48; 177), sepsis (111), critically ill (34), cirrhosis (126), chemotherapy (157), disuse (17) and denervation (119). Together, the above findings in normal and diseased muscle clearly indicate that a proper balance of the autophagic flux is essential for maintaining healthy skeletal muscle, and that unbalanced autophagy is a main pathogenic mechanism in many muscle diseases.

2.2.3 Regulation of autophagy in Skeletal Muscles

Inhibitors and activators of the autophagic process determine the amount of newly formed autophagosomes and the maturation and fusion of these autophagosomes with lysosomes thus ensuring that this process is under stringent regulation. Unlike other tissues, in response to different autophagy inducing stimuli, skeletal muscles produce autophagosomes at a sustained rate lasting a number of days (109). Thus, regulation is required at the transcriptional level to replenish LC3, GABARAP and other proteins which are degraded during the fusion process.

In skeletal muscles, this transcriptional regulation is mediated by Forkhead box O (Foxo) class of transcription factors, a subfamily of the large group of forkhead transcription factors. Mammalian cells contain three members of this family, FoxO1 (FKHR), FoxO3 (FKHRL1), and FoxO4 (AFX) (167). AKT, a component of the IGF-1/PI3K/AKT pathway that promotes cell survival and muscle hypertrophy, blocks the function of all three by phosphorylation of three conserved residues, leading to their sequestration in the cytoplasm away from target genes (18).

When activated, FoxOs can induce the expression of genes involved in autophagy as well as ubiquitin-proteosomal pathway. FoxO3 have been implicated heavily in inducing muscle atrophy by promoting the expression of atrogenes like atrogin-1 and MuRF-1 and a number of autophagy-related genes including LC3, GABARAPl 1, Bnip3,Vps34, Ulk1, Atg12, and Atg4B

in mouse muscle in response to fasting and denervation (98; 185). Expression of constitutively active FoxO3 induces autophagy in skeletal muscle (98), and FoxO3 binds directly to the promoter region of the LC3 gene in muscle from fasted mice (98). FoxO1 transgenic mice show markedly reduced muscle mass and fiber atrophy, further supporting the notion that FoxO proteins are sufficient to promote muscle loss (69; 160). In contrast, FoxO knockdown by RNAi can block the upregulation of atrogin-1 expression during atrophy and muscle loss (94; 143). The protein Bnip3 has been shown to interact with LC3 and selectively remove Endoplasmic Reticulum and mitochondria via autophagy, a process known as mitophagy (57; 184). Bnip3 is thought to play a major role in mediating the effect of FoxO3 on autophagy, as Bnip3 knockdown can markedly reduce the induction of autophagy caused by expression of constitutively active FoxO3 in mouse skeletal muscle (98).

Another important activator of autophagy in skeletal muscles is the energy sensor protein AMPK. It is a serine threonine kinase that is activated by cellular energy level. When cellular energy levels are low, AMPK promotes ATP production by switching off ATP-consuming process such as protein synthesis and switching on catabolic pathways such as muscle proteolysis and autophagy (139). AMPK activation has been shown to activate FoxO transcription factors (118). In C2C12 myotubes, which is an *in vitro* murine model for skeletal muscle, AMPK activation by the pharmalogical compound AICAR causes activation and accumulation of FoxO3 in the nucleus (140). Under nutrient deprivation, AMPK activation and mTORC1 inhibition trigger ULK1 complex to associate with AMPK and to dissociate from mTORC1. These changes lead to overall reductions in ULK1 phosphorylation followed by ULK1 kinase activation and initiation of autophagy (38).

Counteracting the effects of autophagy activators are autophagy suppressors. Few autophagy suppressors have been reported, the first of which was Runx1. In response to denervation, Runx1 is upregulated and its inactivation results in excessive autophagy during denervation which leads to severe atrophy (172). Another negative regulator of autophagy in muscle cells is the phosphatase Jumpy. Jumpy blocks autophagosome formation by reducing the levels of PI3P and therefore counteracting the action of the class III PI3 kinase,VPS34(170).

The mTOR and the PI3K/AKT pathways serve as other negative regulators of the autophagic process. mTOR (mammalian target of rapamycin) is an important signalling molecule that regulates diverse cellular functions such as initiation of mRNA translation, cell growth and proliferation, ribosome biogenesis, transcription, cytoskeletal reorganization, long-term potentiation and autophagy (144). mTOR is a negative regulator of autophagy (88). mTOR pathway has two components, the rapamycin-sensitive mTOR complex 1 (mTORC1) which regulates autophagy and consist mTOR catalytic subunit, raptor (regulatory associated protein of mTOR, GβL (G protein β-subunit-like protein) and PRAS40 (proline-rich Akt substrate of 40KDa) (88) and the mTOR complex 2 (mTORC2) consisting of mTOR, rictor (rapamycin insensitive companion of mTOR), GβL**,** SIN1 (SAPK interacting protein 1) and PROTOR (protein observed with rictor) that is not a direct autophagy regulator (180). mTORC1 is inhibited under conditions of nutrient, specifically amino acid deprivation (75) thereby downregulating protein synthesis pathways and activating autophagy (105). Phamracologically inhibiting mTOR with rapamycing also triggers autophagy (155). The focal point of mTOR mediated regulation of autophagy is the ULK-1/Atg-13/FIP200 initiator complex of autophagy. Under nutrient-rich conditions, mTORC1 suppresses autophagy through direct interaction with this complex and mediates phosphorylation-dependant inhibition of the kinase activities of

Atg13 and ULK-1(77). When mTORC1 is inhibited either by amino acid deprivation or rapamycin treatment, mTORC1 dissociates from this complex, thus leading to a dephosphorylation dependant activation of ULK-1 and ULK-1 mediated phosphorylations of Atg13, FIP200 and ULK-1 itself (61; 153). In skeletal muscles, mTOR is essential for muscle hypertrophy, since treatment with rapamycin completely blocks the muscle growth of adult or regenerating myofibers (16; 120). However, the role of mTOR in autophagy regulation appears to be much less important as rapamycin-mediated mTOR inhibition only increases protein breakdown by as little as 10% in cultured myotubes and even *in vivo* inhibition using rapamycin or RNAi mediated deletion of mTOR is not sufficient to induce atrophy and autophagosome formation (98; 185). In fact, deletion of mTOR gene specifically in skeletal muscles leads to muscular dystrophy rather than atrophy (133).

The PI3K/AKT pathway is another negative regulator of autophagy in skeletal muscles (141). It must be noted that the Class I PI3Kinase and Class III PI3K exert opposite effects on autophagy (123). The binding of growth factors or insulin to cell surface receptors activates the Class Ia PI3K. Activated Class Ia PI3 Kinase then converts the plasma membrane lipid phosphatidylinositol-3,4,5-bisphosphate (PIP_2) to phosphatidylinositol-3,4,5-trisphosphate (PIP_3), which in turn recruits phosphoinositide-dependant kinase 1 (PDK1) and Akt/PKB to the plasma membrane (20). Akt is activated by its phosphorylation on two sites: the mTORC2 mediated phosphorylation on Ser-473 (145) and the phosphorylation by PDK1 on the activation loop of Akt on Thr-308.

Activated Akt feeds forward and activates mTORC1. Activation of Akt results in the phosphorylation of proteins in the tuberous sclerosis complex (TSC). This has an inhibitory affect on TSC. The TSC proteins include a GTPase-activating protein (GAP) which inactivates

Rheb. Rheb is a potent activator of mTORC1 (84; 99). Thus Akt can sustain mTORC1 activation.

However, to keep the system in check, mTORC1 plays a negative feedback regulation on the PI3K-Akt pathway. It was observed that upon rapamycin treatment, mTOR and its downstream mediator p70S6K is inhibited. This relieves the inhibitory effect of p70S6K phosphorylation on insulin receptor substrate -1 (IRS-1). IRS-1 is a key adaptor protein in mediating insulin and insulin-like growth factor-1 (IGF-1) signaling and downstream PI3K/Akt activation (154). This complex series of regulatory mechanisms have had implications in a wide range of biological processes such as cell survival, tumourigenesis, cell growth etc. However, their importance in autophagy requires further clarification.

Recent evidence has shown that PI3K/Akt pathway is perhaps the most powerful regulator of autophagy in skeletal muscles. Acute activation of Akt in adult mice or in muscle cell cultures completely inhibits autophagosome formation and lysosomal-dependent protein degradation during fasting (98; 185; 186). Akt inhibition also causes a 50% increase in protein degradation (185). AKT inhibits autophagy through several mechanisms. First, AKT phosphorylates and inhibits tuberous sclerosis complex-2, thereby activating the mTORC1 complex and inhibiting ULK1 kinase activity (99). Second, AKT inhibits autophagy through inactivation of FOXO transcription factors, which as described previously, play critical roles in maintaining autophagy by regulating transcription of several short-lived proteins that are consumed during autophagosome-lysosome fusion, including LC3B, GABARAPL1, and BNIP3. Lastly, AKT also inhibits autophagy by phosphorylating beclin and enhancing beclin interactions with 14-3-3 protein and vimentin, a type III intermediate filament protein, thereby limiting

Beclin availability for the formation of the Beclin complex, which is necessary for autophagosome formation (171).

2.3 Reactive Oxygen Species

Reactive oxygen species are formed inside cells due to incomplete reduction of oxygen (8). ROS are derived mainly from mitochondrial oxidative phosphorylation, however, other sources including NADPH oxidase, xanthine oxidase, glucose oxidase and other oxidoreductases may contribute to cellular ROS production (129). Generation of ATP in the mitochondria requires the transport of protons across the inner mitochondrial membrane by means of an electron transport chain. In the electron transport chain, electrons are passed through a series of macromolecular complex of proteins via a succession of oxidation-reduction reaction. The last destination for the electron along this chain is an oxygen molecule, which gets reduced to water (8). However, a certain percentage of electrons (around 0.15% by recent estimates (161)) is instead prematurely and incompletely reduced, giving rise to the superoxide radical ($\cdot O_2^-$). This is a highly reactive species and along with the secondary reactive oxygen species it generates such as perhydroxyl radical and peroxynitrite, causes damage to proteins, lipids and DNA directly (176). The superoxide anion is however, quite unstable and undergoes either sponstaneous or enzymatic dismutation to generate hydrogen peroxide (51). These dismutation reactions are carried out by Manganese Superoxide Dismutase (MnSOD) enzyme in the mitochdondria and Copper or Zinc Superoxide Dismutase (CuZnSOD) enzyme in the cytoplasm (19).

Hydrogen peroxide (H_2O_2) is a nonradical and serves as a weak oxidant with a relatively long half-life allowing its diffusion within cells and across membranes (52) and reacts with many different cellular molecules and activates a wide number of signalling pathways. Moreover, H_2O_2 sometimes undergoes Fenton chemistry in the presence of free iron or other transition metal ions which can give rise to a highly reactive hydroxyl radical (169). This entity reacts immediately with any surrounding biomolecules, exerting most of the deleterious effects associated with oxidative stress. To protect the cells from such oxidative damage, cells have developed a network of effective antioxidant mechanisms. Catalase and glutathione peroxidase enzymes break down H_2O_2 into water. Soluble antioxidants such as glutathione molecule act as a substrate for the enzyme action that breaks down hydrogen peroxide into water (47). Peroxiredoxins (Prxs) are another class of antioxidants which use a conserved Cys residue to reduce peroxides (54).

However, recent evidence has shown ROS to be involved in cellular signalling. Although their reactive nature might seem to make them indiscriminate towards their targets, ROS operates in signalling through chemical reactions with specific atoms of target proteins that lead to covalent protein modifications (117). The oxidative interface consists mainly of the redox regulation of redox-reactive cysteine (Cys) residues on proteins by ROS (66). Oxidation of these residues leads to the formation of disulphide bonds with nearby cysteines. These oxidative modifications result in changes in structure and/or function of the protein, which are then reversed by the action of antioxidants.

There are many mechanisms by which ROS directly interacts with critical signalling molecules to regulate in a broad variety of cellular processes. ROS has been shown to play an important role in controlling the activities of many kinases. The nutrient sensitive Raptor-mTOR pathway is activated by presence of oxidizing agents (146). Other kinases influenced by ROS

include MAP kinases such as p38 (68; 134), c-Jun N-terminal kinase (JNK) (103) and extracellular signal-regulated kinase 1/2 (ERK 1/2) (30) all of which regulate cell survival and proliferation.. Moreover, many phosphotyrosine phosphatases (PTPs) are regulated by ROS, of which PTEN, the phosphatase responsible for inactivating the PI3K-AKT pathway is of particular importance (85; 152). ROS has been shown to oxidise and inactivate PTEN, thus promoting Akt activation (87). Additionally, ROS plays important roles in other processes such as ROS homeostasis and antioxidant gene regulation such as thioredoxin, peroxiredoxin, Ref-1 (72; 178) and Nrf-2(13); mitochondrial oxidative stress, apoptosis, aging (7); iron homeostasis through iron–sulfur cluster proteins (IRE–IRP) (96) and ATM-regulated DNA damage response (49) among others.

Depending on its efficacy, the antioxidant cellular network plays a primary role in maintaining ROS below a physiologically compatible threshold level, thus allowing ROS to serve, theoretically, as signaling molecules and avoiding them to exert direct toxic effects. However, production of excessive amount of ROS can be exacerbated as a consequence of certain physiological stresses such as starvation, hypoxia, disuse and denervation leading to a condition known as oxidative stress (1).

2.3.1 Reactive Oxygen Species and autophagy

Autophagy is also modulated by ROS (147; 168). Conditions that lead to oxidative stress such as starvation, hypoxia, growth factor deprivation or cytokine expression also lead to autophagy in many different types of cells (23; 36; 79; 183). Relatively high levels of ROS can indirectly induce autophagy by causing endoplasmic reticulum (ER) stress (102), by altering mitochondrial membrane potential (24) , or by recruitment of pro-autophagy proteins such as

BNIP3 and PARKIN (147). Scherz-Shouval et al. showed that ROS regulates autophagy by modulation of the action of Atg4 on LC3 (168). As was previously described, lipidation of LC3 is a crucial step in autophagy induction. Atg4 is a cysteine protease which delipidates LC3-II on the cytosolic surface of autolysomes, thus allowing it to be recycled (182). Under oxidative conditions, Atg4 is oxidised and inactivated, thus allows LC3 to remain lipidated and induce autophagy.

To answer the question of which particular ROS entity is responsible for triggering atuophagy, Chen et al. conducted a study in which specific inhibitors for $\cdot O_2^-$ and H_2O_2 were used in order to elucidate their respective roles in starvation induced autophagy. Consequently, it was shown that the $\cdot O_2^-$ radical was the major ROS regulating autophagy (23)

In another study, Underwood et al. reported that many autophagy inducing stimuli result in the production of ROS and both basal and stimulated autophagy can be blocked by using the exogenous antioxidants *N*-acetyl cysteine, Vitamin E as well as by overexpressing SOD (89) in a neurodegeneration model. This is associated with an impaired clearance of the aggregate-prone proteins associated with neurodegenerative disorders, underlining the important role of played by autophagy in the elimination of such damaging entities.

2.3.2 Mitochondria, ROS and autophagy.

Mitochondria are essential organelles for eukaryotic cells, providing the main site of energy production. Having its own genome, the mitochondria are also an important site for the production of important proteins. The autophagic process has important implications for the mitochondria. The autophagic process is required for the proper recycling of damaged mitochondria. This selective and specific elimination of mitochondria by autophagy is called

mitophagy (181). Parkin, an E3 ubiquitin ligase linked to most recessively inherited familial juvenile Parkinson's diseases is selectively recruited to impaired mitochondria where it promotes their mitophagy (116). This process is particularly important for erythrocyte maturation, where mitochondrial clearance is essential for their proper functioning (150). Moreover, mitochondria itself might regulate autophagy as recently it was shown that mitochondria might provide the membrane source needed for the formation of autophagosomes (53).

Nevertheless, the principle mechanism by which mitochondria influences autophagy is through ROS production. Mitochondria are the primary source of cellular ROS, which under conditions of oxidative stress might be hazardous to their own lipids, proteins and DNA leading to mitochondrial dysfunction (55). Moreover, under starvation conditions, mitochondria lose their membrane potential, release ROS and undergo mitophagy (76).

Many groups have demonstrated that ROS produced by mitochondria are essential for stress-induced autophagy (6; 24; 148). Moreover, recently it was reported that $\cdot O_2^-$ produced specifically from the mitochondria induces autophagy by activation of AMPK, a pro-autophagy regulator (90). These studies show that mitochondrial ROS may affect the cellular signalling involved in regulating autophagy. However, the effect of ROS on other signalling molecules and regulators involved in autophagy has not been properly elucidated. Moreover, how physiological ROS produced by the mitochondria regulates of basal autophagy has not been investigated.

2.3.3 Reactive Oxygen Species and skeletal muscles

In skeletal muscles this phenomenon is quite evident where ROS is produced at relatively low rates in normal resting muscle fibers and exert positive influences on muscle contractility (130-132). This is due to the low level of ROS that activate specific key signalling

molecules such as PGC-1α, AMPK and MAPK which control cellular mechanisms for muscle adaptation including oxidative metabolism, mitochondrial biogenesis and mitochondrial functionality (8). Moreover, low levels of ROS play an important role in inducing upregulation of growth factors such as IGF-1 which leads to muscle hypertrophy (56). However, under pathological conditions, where aberrant increases in ROS production and/or decreases in antioxidants occur, ROS accumulate to produce oxidative stress. Oxidative stress is considered to be deleterious to skeletal muscle tissue since it was shown to play a pathogenic role in numerous inherited muscular dystrophies (114) and was identified as one of the causative agents in various muscle diseases (164). High levels of ROS alters skeletal muscle by inducing mitochondrial dysfunction (14), modifying critical proteins involved in myofilament contraction (9), and by enhancing muscle protein degradation (9; 104).

2.4 ROS, Autophagy and Skeletal Muscle

Regulation of autophagy in skeletal muscles by ROS is still vastly unexplored. Dobrowolny et al. reported that in a transgenic mouse model expressing a mutant version of superoxide dismutase 1 (SOD1) triggers significant induction of autophagy (37). These transgenic mice develop progressive muscle atrophy which is associated with reduction in muscle strength, alterations in contractile apparatus and mitochondrial dysfunction as a consequence of oxidative stress. Recently, Mofarrahi et al reported augmented levels of autophagy in skeletal muscles of mice infected with bacterial lipopolysaccharide (LPS) as shown by the augmented lipidation of LC3-II as well as increased expression of autophagy-related proteins including BECLIN1,p62, PI3KC3, ATG5 and ATG12 (111). Skeletal muscles of these mice undergo severe sepsis induced atrophy. Moreover, LPS mediated sepsis induces

morphological and functional abnormalities in mitochondria and leads to exacerbated ROS production, oxidative stress and inhibition of mitochondrial biogenesis.

Although these results confirm that relatively high levels of ROS have a stimulatory effect on autophagy in skeletal muscles - they do not, however, provide any information as to whether normal physiological levels of ROS produced by muscle cells influence autophagy. Specifically, the source of ROS generation that triggers autophagy as well as the exact mechanism by which ROS and antioxidants can influence the complex regulatory signalling network governing autophagy needs further clarification.

2.5 Aims of the Study

We hypothesize those physiological levels of mitochondrial ROS production in skeletal muscles play an important functioning role in promoting basal autophagy and that enhanced mitochondrial ROS levels, released in response to acute starvation or amino acid deprivation induce further autophagy under these conditions. We also hypothesize that physiological levels of mitochondrial ROS production promote skeletal muscle autophagy in part by altering he balance between activities of mTORC1and AMPK and their effects on ULK-1 phosphorylation, and in part by selective inhibition of the AKT pathway.

SECTION 3 – MATERIALS AND METHODS

3.1 MATERIALS

C2C12 myoblasts were obtained from the American Type Culture Collection, (ATCC, Manassas, VA). Dulbecco's Modified Eagle Medium (DMEM), Earle's Balanced Salt Solution (EBSS), Hank's Balanced Salt Solution (HBSS), fetal bovine serum (FBS), horse serum (HS), the antibiotic gentamicin, MitoSOX™ Red reagent, and a Superscript® IIH Reverse Transcriptase Kit were all obtained from Invitrogen Canada, Inc. (Burlington, ON). The antioxidants tempol (4-Hydroxy-2,2,6,6-tetramethylpiperidinyloxy,) and mito-tempol ((2-(2,2,6,6-tetramethylpiperidin-1-oxyl-4-ylamino)-2-oxoethyl)triphenylphosphonium chloride monohydrate) were obtained from Enzo LifeSciences (Brockville, ON). NAC was obtained from Alfa Aesar (Ward Hill, MA). The peptides SS31 and SS20 were generously provided by Dr. P. Schiller (Université de Montréal, Montréal). Triciribine hydrate (AKTi), Baf A1, antimycin A and a GenElute™ Mammalian Total RNA Kit were all obtained from Sigma-Aldrich (Oakville, ON). Antibodies for LC3B, phospho-FOXO3A (Ser^{253}), FOXO3A, phospho-AKT (Ser^{473}), AKT, phospho-AKT substrate, phospho-AMPKα (Thr^{172}), AMPKα, phospho-RPS6KB1 (Thr^{389}), RPS6KB1, phospho-ULK1 (Ser^{555}), and ULK1 were obtained from Cell Signaling Technology, Inc. (Danvers, MA). Antibody for SQSTM1 (p62) was obtained from Abnova, Inc. (Walnut, CA). Antibodies for β-TUBULIN and β-ACTIN were obtained from Sigma-Aldrich. SuperSignal™ West Pico Chemiluminescent Substrate (ECL) was obtained from Thermo Fisher Scientific (Rockford, IL).

3.2 METHODS

3.2.1 Cell culture: Murine C2C12 myoblasts were cultured in growth medium (DMEM supplemented with 10% FBS) at 37°C and 5% CO_2. Cells were seeded at 1.5 x 10^5, 8 x 10^4, and

1 x 10^4 on 6-well (34.8mm well diameter), 12-well (22.1mm well diameter) and 96-well (4.26mm well diameter) plates, respectively. Prior to experimental treatment, myoblast differentiation was induced at 80% confluency by incubating cells for 5 days in differentiation medium (DM) (DMEM supplemented with 2% heat-inactivated HS) to form myotubes.

3.2.2 Induction of autophagy: Acute nutrient deprivation was accomplished by replacing DM with an EBSS solution containing glucose, antibiotics, and electrolytes. mTORC1 inhibition was accomplished with 200 ng/ml of rapamycin. Leucine deprivation (Leu(-)) was accomplished by incubating cells with DMEM-LM medium lacking the essential amino acid leucine. For protein and RNA measurements, stimuli were maintained for 1.5 hr. For proteolysis rate measurements, stimuli were maintained for 4 hr (minimum period required to accurately measure proteolysis using [^{3}H] tyrosine release assay).

3.2.3 Antioxidant treatment: In cultured myotubes, tempol was used at 10 mM, NAC at 20 mM, mito-tempol at 500 μM, SS31 and SS20 peptide at 1 μM. Phosphate buffered saline (PBS) was used as vehicle (control) in all protocols except those involving mito-tempol, where dimethyl sulfoxide (DMSO, 0.02%) was used.

3.2.4 Rate of proteolysis: Long-lived protein degradation pulse-chase assays were performed as previously described \(98). To label cell proteins, C2C12 myotubes were incubated for 24 hr in pulse medium containing [^{3}H] tyrosine (4 μCi/ml). Pulse medium was replaced with chase medium containing 2 mM unlabeled tyrosine (with or without antioxidant to prevent re-incorporation of [^{3}H] tyrosine and incubated for 2 hr. Fresh chase medium (with or without EBSS, rapamycin, or leucine deprivation) was added. For the basal rate of proteolysis, 200 μl aliquots were collected at 4 hr intervals for up to 16 hr. For EBSS, rapamycin, and leucine

deprivation, aliquots were collected at hourly intervals for up to a maximum of 4 hr since after that time treatments exert a deleterious effect on cell survival due to the development of severe oxidative stress. Aliquots were combined with 10% TCA to precipitate proteins. Preparations were then centrifuged at 14,000 G for 10 min. Supernatants were collected and radioactivity was measured by liquid scintillation counting. To determine overall radioactivity in cell proteins at end of treatment, cells were solubilized with 2 ml of NaOH (1 N) and radioactivity was measured as above. Acid-soluble radioactivity values reflect the presence of degraded pre-labeled, long-lived proteins at different times and are expressed relative to total initial radioactivity. Values were plotted against time to provide the rate of proteolysis.

3.2.5 Mitochondrial O_2^- production: C2C12 myoblasts ($1x10^4$) were seeded in 96-well black flat bottom microplates. Following five days of differentiation in DM, myotubes were incubated in HBSS buffer containing 5 μM MitoSOX™ Red for 30 min. Myotubes were either untreated (basal mitochondrial O_2^- levels) or treated with EBSS buffer, rapamycin, or antimycin A (control). Leucine deprivation medium interfered with fluorescence signal and hence it was not used in this experiment. Fluorescence was measured using a SpectraMax® M2 Microplate reader at 0, 10, and 15 min. Experiments were also done in the presence of tempol (10 mM), mito-tempol (500 μM) or antimycin A (positive control).

3.2.6 Effects of antioxidants on *in vivo* muscle autophagy: All procedures were approved by the Animal Care Committees of McGill University. Adult (8- to 12-wk-old) male wild-type C57/BL6j mice were fed *ad libitum*. Animals were divided into two groups: Group 1 received an intra-peritoneal injection (i.p.) of vehicle (PBS) and Group 2 received an i.p. injection of NAC (500 mg/kg). Animals were euthanized with sodium pentobarbital 2, 6, or 24 hr after PBS or

NAC injection. Diaphragm (representative of skeletal muscle) was quickly excised, flash-frozen in liquid nitrogen, and stored at -80^{o}C for later use.

3.2.7 In vivo skeletal muscle autophagic flux: Colchicine was used to measure the effects of NAC on basal autophagic flux. Mice were divided into two main groups, a vehicle group that received an i.p. injection of PBS and a colchicine group that received an i.p. injection of colchicine (0.4 mg/kg). Twenty-four hours later, animals in the vehicle group received a second i.p. injection of PBS or NAC (500 mg/kg). Animals in the colchicine group received a second i.p injection of colchicine in combination with PBS or NAC. Twenty-four hours after the second injection, animals were euthanized with sodium pentobarbital, diaphragm was quickly excised, flash-frozen in liquid nitrogen, and stored at -80^{o}C for later use.

3.2.8 RNA extraction and real-time PCR: Total RNA was extracted using a GenElute™ kit. Total RNA (2 μg) was reverse transcribed using a Superscript® IIH Reverse Transcriptase kit and random primers. Reactions were incubated at 42ºC for 50 min and at 90ºC for 5 min. Real-time PCR detection of mRNA expression was performed using a Prism® H7000 Sequence Detection System. Expressions of autophagy-related genes *LC3B*, *Gabarapl1*, *Bnip3* were quantified using specific sets of primers (Table 1). Expressions of two muscle-specific E3 ligases (*Atrogin-1* and *MuRF1*) were also quantified (Table 1). In all assays, 1 μl of reverse-transcriptase reagent was added to 25 μl of SYBR® Green Mastermix and 3.5 μl of 10 μM primer. The thermal profile used was as follows: 95°C for 10 min; 40 cycles each of 95°C for 15 s, 57°C for 30 s, and 72°C for 33 s. All real-time PCR experiments were performed in triplicate. Relative mRNA level quantifications of target genes were determined using the threshold cycle ($\Delta\Delta C_T$) method using the housekeeping gene *β-Actin*.

3.2.9 Immunoblotting: C2C12 myotubes were washed twice with PBS and lysed using lysis buffer (pH 7.5) containing 50 mM HEPES, 150 mM NaCl, 100 mM sodium fluoride, 1 mM sodium orthovanadate, 5 mM EDTA, 1 mM PMSF, 2 μg/ml leupeptin, 5 μg/ml aprotinin and 0.5% Triton® X-100. Cell debris and nuclei were separated by centrifugation at 5,000g for 5 min. Supernatants were boiled for 5 min then loaded onto tris-glycine SDS polyacrylamide gels. Proteins were electrophoretically transferred onto PVDF membranes, blocked for with 5% non-fat dry milk, and incubated overnight with primary antibodies at 4°C. Membranes were washed and incubated with HRP-conjugated secondary antibody. Specific proteins were detected with an enhanced chemiluminescence (ECL) kit. Equal loading of proteins was confirmed by stripping membranes and re-probing with anti-β-TUBULIN or β-ACTIN antibodies. Blots were scanned with an imaging densitometer and optical densities (OD) of protein bands were quantified using a Gel-Pro Analyzer (Media Cybernetics). Changes in the levels of phosphorylation of a given protein were quantified as the ratio between phosphorylated and total protein optical densities. To quantify LC3B levels, a standard curve consisting of purified LC3B protein was run alongside the same gel (0.4-1.2 ng). LC3B protein density was converted to LC3B protein quantity by extrapolation from the standard curve using regression analysis tools. These values were then normalized to μg of total muscle protein loaded per lane. LC3B autophagic flux was quantified as the difference between LC3B-II values measured in the absence and presence of colchicine or Baf A1, as described by Haspel *et al*(59).

3.2.10 Data analysis: Results are shown as means ± SEM. For immunoblotting experiments, at least three independent measurements were performed for each experimental treatment. Eight independent measurements of rate of proteolysis, mRNA expression, and MitoSOX™ Red

fluorescence were performed. Comparisons between different groups were performed with Student t-tests where probability (P) values of less than 0.05 were considered significant.

SECTION 4 – RESULTS

ROS regulation of rate of proteolysis: We measured long-lived protein degradation in differentiated C2C12 myotubes under basal condition and in response to three physiological stimuli known to induce autophagy, namely, acute nutrient deprivation, inhibition of mTORC1 and deprivation of the amino acid leucine. Figure 1 illustrates that long-lived protein degradation rates significantly increased after 4 hr incubation in Earle's Balanced Salt Solution (EBSS), rapamycin treatment, or leucine deprivation (Figure 1A). To assess the role of endogenous ROS in the regulation of proteolysis in C2C12 myotubes, we used the antioxidants tempol and N-acetyl cysteine (NAC). Tempol is a membrane permeable piperidine nitroxide that mimics SOD by dismuting O_2^- anions. It also detoxifies redox-reactive transition metal ions, and directly reacts with many ROS-forming adducts (12; 137; 138). NAC is a precursor of the cellular antioxidant glutathione (2). Pre-incubation with the antioxidant tempol (superoxide dismutase mimic) for 24hr significantly attenuated the basal rate of proteolysis, as well as the rates induced by EBSS, rapamycin, and Leu(-) (Figure 1A). Basal and EBSS-induced proteolysis are also significantly attenuated by pre-incubation with tempol for 2 hr (Figure 1B). Pre-incubation with NAC for 30 min exerted no effect on the basal rate of proteolysis but significantly attenuated EBSS-induced proteolysis (Figure 1B).

LC3B lipidation and LC3B flux: Under basal conditions, LC3B-I (free form) intensity is significantly higher than that of the lipidated form (LC3B-II) in myotubes pre-incubated with vehicle (phosphate buffered saline, PBS) (Figure 2A). Incubation with EBSS, rapamycin treatment, or leucine deprivation for 1.5 hr resulted in significant increases in LC3B-II intensity

and augmentation of LC3B-II/LC3B-I ratios (Figure 2A-B). In myotubes pre-incubated with tempol, neither EBSS, Rapa, nor Leu(-) exerted any effect on LC3B-II protein intensity or LC3B-II/LC3B-I ratio compared to basal condition (Figure 2C-D). Under basal conditions, in myotubes pre-incubated with tempol for 24 hr or pre-treated with NAC for 30 min, intensities of LC3B-I, LC3B-II, and SQSTM1 (p62) were significantly greater than those observed in myotubes pre-incubated with vehicle (PBS) (Figure 2 E). Similar observations were made when myotubes were pre-incubated with tempol for 2 hr (results not shown). These results suggest that antioxidants trigger the accumulation of autophagosomes, which may be a result of either increased synthesis or decreased degradation. Therefore, the effects of antioxidants on LC3B protein intensity under basal conditions and in response to EBSS in the absence and presence of the lysosomal inhibitor bafilomycin A1 (Baf A1) were assessed. Baf A1 (200 nM) was administered 1 hr prior to cell lysis. In the absence of Baf A1, significantly greater intensities of LC3B-I, LC3B-II, and SQSTM1 were observed in myotubes pre-incubated with tempol for 24 hr as compared to those pre-incubated with vehicle (Figure 2F). In the presence of Baf A1, higher of LC3B-I, LC3B-II and SQSTM1 intensities were observed in myotubes under basal conditions and in those pre-incubated with EBSS (Figure 2F). LC3B-II autophagic flux values under basal conditions and in response to EBSS exposure were significantly lower in cells pre-incubated with tempol as compared to those pre-incubated with vehicle (Figure 2G).

Transcriptional regulation of autophagy-related genes: To assess whether endogenous ROS regulate autophagy-related gene expressions, mRNA levels of *Lc3bB*, *Gabarapl1* and *Bnip3* were measured. These genes are regulated mainly by the FOXO transcription factors (185). Expressions of two muscle-specific E3 ligases (*Atrogin-1* and *MuRF1*), which are critical to proteasome pathway, were also measured. In myotubes pre-incubated with vehicle, EBSS,

rapamycin, and Leu(-) elicited significant increases in mRNA expressions of *Lc3b*, *Gabarapl1*, *Bnip3*, *Atrogin-1*, and *MuRF1* (Figure 3). However, in cells pre-incubated with tempol, neither EBSS, rapamycin, nor Leu(-) induced significant increases in the expressions of *Lc3b*, *Gabarapl1*, *Bnip3*, or *Atrogin-1* and the relative induction of *MuRF1* that was observed was significantly lower than that observed in cells pre-incubated with vehicle. These results indicate that, in response to atrophic stimuli, antioxidants not only block autophagosome degradation but also impair autophagy-related gene expressions.

ROS and *in vivo* skeletal muscle autophagy: Effects of endogenous ROS on the regulation of *in vivo* basal autophagy were assessed by administering NAC in mice and measuring changes in LC3B and SQSTM1 protein intensities. The diaphragm was used as a representative skeletal muscle. Within 6 hr, intraperitoneal NAC injection elicited significant increases in the intensities of LC3B-I, LCB-II, and SQSTM1 protein bands as compared to vehicle injection (PBS) (Figure 4A-B). This pattern is similar to that observed in myotubes pre-incubated with tempol or NAC (Figure 2). To assess whether increases in LC3B and SQSTM1 intensities were due to enhanced autophagy or reduced degradation, *in vivo* flux measurement were performed by pre-injecting colchicine into animals that were subsequently injected with PBS or NAC. Basal LC3B-II autophagic flux was significantly lower in animals that received NAC injection as compared to those that received vehicle (Figure 4).

Mitochondria-derived ROS and the regulation of autophagy: To confirm that mitochondria are the major sources of endogenous ROS that regulate autophagy in skeletal muscles, we first measured mitochondrial ROS levels using the fluorescent dye MitoSOX™. This dye permeates live cells where it selectively targets mitochondria and is rapidly oxidized by O_2^-, but not by other ROS (113). We also used two mitochondrial-specific antioxidants, mito-tempol and SS31

peptide. Mito-tempol is a derivative of tempol with similar antioxidant properties to those exhibited by tempol (93). The peptide SS31 is a cell-permeable tetrapeptide (d-Arg-2′, 6′-dimethyltyrosine-Lys-Phe-NH_2) targeted to the inner mitochondrial membrane that exerts strong antioxidant capabilities. It reduces mitochondrial ROS levels, prevents mitochondrial swelling, and guards against oxidative cell death (187). The peptide SS20 (Phe-D-Arg-Phe-Lys-NH_2) does not exert antioxidant activity and is generally used as a control for SS31 (187).

MitoSOX™ Red fluorescence progressively and significantly increased in response to EBSS, rapamycin, and antimycin A (Figure 5A-B). Pre-incubation with mito-tempol significantly attenuated EBSS-, rapamycin- and antimycin A-induced fluorescent signals (Figure 5A-B). Antimycin A, inhibitor of complex III, was used here as a positive control to detect enhanced mitochondrial ROS levels. Pre-incubation with tempol also resulted in the attenuation of fluorescence, but to a lesser extent than that elicited by mito-tempol (Figure 5A-B). Figure 5C-D indicates that pre-incubation with mito-tempol or SS31 peptide strongly and significantly inhibited the basal rate of proteolysis and in response to EBSS, rapamycin, and Leu(-). EBSS, rapamycin, and Leu(-) significantly increased LC3B-II protein levels and LC3B-II/LC3B-I ratios in myotubes pre-incubated with vehicle (DMSO) (Figure 5E-F). This response was not seen in myotubes pre-incubated with mito-tempol (Figure 5E-F).

Roles of ROS in ULK1 phosphorylation and autophagy initiation: In myotubes pre-incubated with vehicle, phosphorylation of AMPKα on Thr^{172} was not affected by EBSS, rapamycin, or Leu(-) (Figure 6A-B). Pre-incubation with tempol significantly attenuated AMPK phosphorylation at the basal level and in response to EBSS, rapamycin, and Leu(-) (Figure 6A-B). This response was also observed in myotubes pre-incubated with NAC and in the diaphragm of mice injected with NAC (supplementary materials).

In myotubes pre-incubated with vehicle, phosphorylation of RPS6KB1 on Thr^{389} (an mTORC1-specific activation site) significantly decreased in response to EBSS, rapamycin, and Leu(-), confirming that that these stimuli significantly attenuate mTORC1 activity (Figure 6C-D). In myotubes pre-incubated with tempol, phosphorylation of RPS6KB1 on Thr^{389} was significantly lower under basal conditions of vehicle pre-incubation (Figure 6C-D). In myotubes pre-incubated with tempol, RPS6KB phosphorylation levels in response to EBSS, rapamycin, and Leu(-) were similar to those measured with vehicle pre-incubation (Figure 6C-D). Similar results were obtained with NAC and mito-tempol pre-incubation (supplementary materials).

Figure 6E-F illustrates changes in total and phosphorylated ULK1 (Ser^{555}) protein levels in myotubes pre-incubated with vehicle or tempol. In myotubes pre-incubated with vehicle, phosphorylation of ULK1 on Ser^{555}, but not total ULK1 levels, were significantly attenuated by EBSS, rapamycin, and Leu(-) (Figure 6). Similarly, in myotubes pre-incubated with tempol, ULK1 phosphorylation was significantly attenuated by all three treatments (Figure 6). Pre-incubation with tempol exerted no effect on basal ULK1 phosphorylation when compared to pre-incubation with vehicle.

ROS regulation of AKT phosphorylation: In myotubes pre-incubated with vehicle, incubation with EBSS for 1.5 hr substantially reduced AKT phosphorylation on Ser^{473} (Figure 7A-B). In comparison, rapamycin and Leu(-) caused significant increases in AKT phosphorylation as compared to basal levels (Figure 6A-B). In myotubes pre-incubated with tempol, a significant increase in AKT phosphorylation was observed at the basal level and in response to EBSS, rapamycin, and Leu(-) when compared to cells pre-incubated with vehicle (Figure 7A-B). Similar results were observed in cells pre-incubated with NAC (Figure 7C). To confirm that the observed rise in AKT phosphorylation in response to tempol or NAC was associated with

increased AKT activity, immunoblotting was performed using a phospho-AKT substrate antibody. Under basal conditions and in response to EBSS, rapamycin, and Leu(-), intensities of several protein bands were increased in myotubes pre-incubated with tempol as compared to those pre-incubated with vehicle (Figure 7D).

Phosphorylation of the transcription factor FOXO3A, a known target of AKT and a regulator of autophagy-related genes, was also measured (185). In myotubes pre-incubated with tempol, phosphorylation of FOXO3A on Ser^{253} increased under basal conditions and in response to EBSS, rapamycin, and Leu(-) as compared to cells pre-incubated with vehicle. These results confirm that antioxidant-induced augmentation of AKT phosphorylation is associated with enhanced FOXO3A phosphorylation.

The importance of AKT to antioxidant inhibition of muscle autophagy was evaluated using a selective AKT inhibitor (triciribine, AKTi). We reasoned that if ROS promote autophagy in muscle cells, in part through inhibition of AKT, then antioxidants will fail to inhibit autophagy when combined with an AKT inhibitor such as AKTi. Incubation of C2C12 myotubes with AKTi (20 μM) eliminated AKT phosphorylation confirming the potency of this compound (supplementary materials). Under basal conditions, AKTi exposure significantly increased the rate of proteolysis, confirming that AKT inhibits autophagy (Figure 8A). Pre-incubation with tempol, mito-tempol, or SS31 significantly attenuated basal proteolysis rates, confirming that mitochondrial ROS promote basal autophagy (Figure 8). This antioxidant-triggered inhibition of basal proteolysis rates did not occur in the presence of ATKi (Figure 8).

In myotubes pre-incubated with vehicle, AKTi triggered a significant increase in the LC3B-II/LC3B-I ratio, confirming that AKT inhibition increases basal autophagy (Figure 8).

Interestingly, a similar response to AKTi was observed in myotubes pre-incubated with tempol, indicating that tempol does not attenuate autophagy when AKTi is present. Collectively, these results indicate that active AKT is required for inhibition of basal proteolysis by antioxidants (Figure 8).

Myotubes were pre-incubated with vehicle, tempol, or tempol plus AKTi. Pre-incubation with tempol resulted in significant inhibition of EBSS-, rapamycin- and Leu(-)-deprivation-induced proteolysis as compared to cells pre-incubated with vehicle (Figure 8). Inhibition of EBSS-induced proteolysis still occurred in the presence of ATKi, but did not with respect to rapamycin- and Leu(-) (Figure 8). These results highlight the importance of AKT in endogenous ROS regulation of autophagy, not only under basal conditions, but also in response to mTORC1 inhibition.

SECTION 5 – DISCUSSION

ROS regulation of skeletal muscle autophagy: This study introduces several novel aspects of ROS regulation of autophagy in skeletal muscles. The first major finding is that endogenous ROS production promotes autophagy at the basal level and in response to acute nutrient starvation and mTORC1 inhibition. In this study, we focused on the regulation of autophagy by basal physiological or endogenous levels of ROS in skeletal muscle cells. To this end, we used antioxidants as a tool to reduce ROS levels in cultured C2C12 myotubes and in intact muscles in vivo. We quantified autophagy using three methods: a long-lived protein degradation assay, LC3B lipidation and LC3B flux, and measurements of autophagy-related gene expression.

Using long-lived degradation assays, we found that pre-incubation with tempol for 24 or 4 hr significantly reduced the basal rate of proteolysis in myotubes (Figure 1). Tempol treatment also led to an increase in the levels of free and lipidated forms of LC3B protein and augmented SQSTM1 protein levels (Figure 2E). Autophagic flux measurements revealed that these changes in LC3B and SQSTM1 are due to the accumulation of autophagosomes. Together, these observations demonstrate that endogenous ROS generation, both at the basal level and in response to relatively short periods of nutrient deprivation or mTORC1 inhibition, promote autophagy in skeletal muscle cells. Our choice of using relatively short periods (1.5 to 4 hr) of acute nutrient deprivation, rapamycin treatment, and leucine deprivation was designed to avoid the development of severe oxidative stress. To our knowledge, this is the first evidence that endogenous, physiological ROS production is an important regulator of autophagy in skeletal muscles. Basal autophagy is thought to be a protective mechanism, responsible for recycling damaged or dysfunctional organelles and protein aggregates, and is known to be critically important to muscle homeostasis (100). We propose here that, under basal conditions,

physiological levels of skeletal muscle cell ROS production promote muscle function not only by enhancing myofilament contractile force, as previously shown (131), but by promoting autophagy.

Our study also demonstrates that acute nutrient deprivation, rapamycin treatment, and leucine deprivation enhances mRNA expressions of autophagy related genes (*Lc3b*, *Gabarapl1*, *Bnip3*) (Figure 3). This finding supports the notion that a transcriptional program involving FOXO transcription factors, is activated in response to atrophic stimuli in skeletal muscles and that this program is designed to replenish the short-lived autophagy-related proteins (LC3B, GABARAPL1, BNIP3) that are required to sustain autophagosome formation (98; 111). Our observation that this increase in autophagy-related gene expression is eliminated by antioxidants (Figure 3) indicates that endogenous ROS promote autophagy in skeletal muscles by activating both non-transcriptional and transcriptional mechanisms designed to initiate and maintain autophagy. These mechanisms are discussed in more detail below.

The nature of ROS that regulate autophagy is unclear. Chen *et al*. concluded that O_2^- anions are the primary regulators of starvation-induced autophagy in HeLa cells based on observations that: autophagy triggered by serum, glucose, or glutamine starvation is associated with increased O_2^- anion levels; autophagy triggered by amino acid starvation is associated with increased O_2^- anion and H_2O_2 levels; and overexpression of SOD2 significantly reduces autophagy, attenuates O_2^- anion levels, and increases H_2O_2 concentrations (23). In this study, we observed that tempol, which exerts its effects mainly by scavenging O_2^- anions, significantly attenuates basal proteolysis rates but NAC does not, suggesting that O_2^- anions may be more important regulators of basal autophagy in C2C12 myotubes than are other ROS (Figure 1). In comparison, nutrient deprivation-, rapamycin treatment- or leucine deprivation-induced autophagy was equally

inhibited by tempol and NAC, suggesting that both O_2^- anions and H_2O_2 may be involved in the regulation of autophagy under these conditions. Further studies are required to elucidate the differential regulatory roles of ROS in skeletal muscles.

Mitochondrial ROS regulation of autophagy: The importance of mitochondrially-derived oxidative stress as a root cause of mitochondrial injury and dysfunction has been well established and recent studies have identified alterations in mitochondrial membrane potentials as an important trigger for mitochondrial recycling by autophagy, a process known as mitophagy (181). The functional roles of mitochondria-derived ROS as regulators of autophagosome formation, however, are unclear. Scherz-Shouval *et al*. observed that starvation in CHO cells and MEFs enhances autophagy and H_2O_2 production and that NAC attenuates both responses (148). They proposed that mitochondrial ROS may be responsible for starvation-induced autophagy. Mammucari *et al*. identified BNIP3, a protein that mobilizes to the mitochondria in response to starvation, as a major regulator of autophagy in intact skeletal muscles (98). A subsequent study by the same group identified alterations in mitochondrial biogenesis and fragmentation as important stimuli for autophagy in skeletal muscles (135). These findings suggest that mitochondria are both a trigger for, and a target of, autophagy in skeletal muscles.

Our study reveals for the first time that in skeletal muscle cells mitochondria-derived ROS are important regulators of basal autophagy and autophagy triggered by acute nutrient deprivation, mTORC1 inhibition by rapamycin, and leucine deprivation. This conclusion is based on two main findings. Firstly, mitochondrial ROS release is significantly elevated in response to nutrient deprivation and rapamycin treatment and this response is attenuated by mito-tempol (Figure 2). Interestingly, we found that tempol itself was also able to reduce the fluorescent signal, albeit less efficiently than mito-tempol, suggesting that tempol may diffuse

into the mitochondria (Figure 2). Secondly, proteolysis rates and LC3B lipidation are strongly attenuated by mito-tempol and SS31 peptide (Figure 4). We should emphasize that this study does not rule out the involvement of ROS other than those that are mitochondrially-derived in the regulation of basal and stress-induced autophagy.

Mechanisms through which ROS regulate autophagy: The exact mechanisms through which mitochondria-derived ROS regulate autophagy remain under investigation. Excessive ROS levels can influence autophagy indirectly by inducing ER stress which, in turn, induces autophagy (102). Oxidative stress can also induce significant mitochondrial damage and accumulation of oxidized protein aggregates, which, by itself, induces autophagy (73). Little information is as yet available as to how physiological levels of ROS affect autophagy and autophagosome formation. Recently, Scherz-Shouval *et al.* used NAC to identify the protease ATG4 as a direct target of ROS action in CHO and HEK293 cells (148). ATG4 cleaves the c-terminus on ATG8 family ubiquitin-like proteins (LC3, GABARAP, and GATE-16) as a prerequisite to their conjugation to phosphatidyl ethanolamine on autophagosome membranes. ATG4 is also involved in delipidation of ATG8 proteins from mature autophagosomes. Scherz-Shouval et al. observed that 30 min of starvation causes significant production of ROS that oxidize a specific cysteine on ATG4, leading to inhibition of the delipidation process without influencing its c-terminus cleavage activity.

The current study does not exclude the possibility that post-translational modification of ATG4 is an important mechanism through which mitochondria-derived ROS regulate autophagy in skeletal muscles. However, in this study we specifically explored ROS as potential regulators of autophagosome initiation. The ULK1-ATG13-FIP200 protein complex has emerged as an important regulator of autophagosome initiation. This complex is under the control of the AMPK

and mTORC1 pathways, particularly in response to cellular starvation. Under normal nutrient supply conditions, mTORC1 associates with the ULK1-ATG13-FIP200 complex through direct interactions between RAPTOR and ULK1; active mTORC1 phosphorylates ULK1 and ATG13, thereby inhibiting ULK1 kinase activity (43; 61; 67). When cells are starved, mTORC1 activity is inhibited and both ULK1 and ATG13 are rapidly de-phosphorylated. Shang *et al.* recently identified thirteen serine and threonine residues in human ULK1, including Ser^{556}, whose phosphorylation declines significantly in response to starvation or mTORC1 inhibition (153). Activation of ULK1 that results from removal of the inhibitory effect of mTORC1 triggers ULK1-mediated activation of FIP200 and ATG13, followed by translocation of the entire ULK1-ATG13-FIP200 complex to the pre-autophagosome membrane, resulting in activation of autophagy (67). AMPK activates autophagy through two mechanisms, namely, direct phosphorylation of ULK1 on several residues, including Ser^{317} and Ser^{777} (77), and activation of ULK1 kinase activity (77). In addition, AMPK directly phosphorylates RAPTOR and inhibits mTORC1 activation, thereby removing the inhibitory effect on ULK1(86). ULK1 activation, therefore, is controlled via a two-pronged mechanism that includes energy sensing (AMPK) and amino acid sensing (mTORC1).

This study highlights two important observations regarding the interplay between AMPK and mTORC1 in relation to autophagy regulation. First, we observed that tempol and NAC significantly attenuate AMPKα phosphorylation on Thr^{172} at the basal level and in response to nutrient deprivation, rapamycin treatment, and leucine deprivation (Figure 5A-B and supplementary materials). These observations suggest that mitochondria-derived ROS in skeletal muscle cells activate AMPK even at the basal level. We speculate that AMPK activation may be an important mechanism through which mitochondria-derived ROS promote autophagy in these

cells. We attempted to measure ULK1 phosphorylation of these residues but commercially available phospho antibodies for Ser^{317} and Ser^{777} residues proved to be inadequate. We should emphasize that a similar link between mitochondrial ROS and AMPK activation has recently been described in response to hypoxia in murine embryonic fibroblasts (39).

Second, we observed that phosphorylation of ULK1 on Ser^{555} declines significantly in response to EBSS, rapamycin treatment, and leucine deprivation (Figure 6). This observation implies that the decline in mTORC1 activity in response to these stimuli triggers dissociation of mTORC1 from ULK1 followed by initiation of autophagy. We recently observed a similar finding in the diaphragm and limb muscles of mice in response to acute starvation (112). The fact that this relative de-phosphorylation of ULK1 on Ser^{555} is also evident in cells pre-incubated with tempol or NAC (Figure 5 and supplementary materials) suggests that dissociation of mTORC1 from ULK1, and possibly activation of ULK1, is not redox sensitive. Further studies are needed to confirm this conclusion.

Role of AKT in ROS regulation of autophagy: Sandri (141) proposed that AKT is a more powerful inhibitor of autophagy in skeletal muscles than mTORC1. This is based on the observation that AKT inhibition elicits stronger induction of autophagy in skeletal muscles than does inhibition of mTORC1 activity with rapamycin (141). Recent evidence suggests that AKT inhibits autophagy through ctivation of mTORC1(99), inactivation of FOXO transcription factors (98) and phosphorylation of BECLIN1 and inhibition of its translocation to autophagosome membranes (171). It is on the basis of these findings that we investigated whether ROS regulation of autophagy in skeletal muscle cells works through modulation of AKT. Our study reveals that AKT phosphorylation on Ser^{473} in cells pre-incubated with tempol or NAC is significantly higher than that observed in cells pre-incubated with vehicle (Figure 6).

This response is independent of mTORC1 activity since it was observed in cells exposed to rapamycin treatment or leucine deprivation, suggesting that endogenous ROS exert an inhibitory effect on AKT activation. This was further confirmed by measuring phosphorylation levels of AKT targets and, more specifically, phosphorylation of the transcription factor FOXO3A, which significantly increases in cells pre-incubated with tempol as compared to cells pre-incubated with vehicle (Figure 7).

The inhibitory effect of endogenous ROS on AKT activation raises an interesting possibility that ROS promote autophagy in skeletal muscles in part through selective inhibition of AKT activity. To test this possibility, we assessed the effects of antioxidants on rates of proteolysis in the absence and presence of a selective AKT inhibitor (triciribine). We found that the inhibitory effect of antioxidants on proteolysis, measured under basal conditions and in response to rapamycin treatment and leucine deprivation, does not take place when AKT is inhibited, nor does the antioxidant effect on LC3B protein accumulation observed in Figure 2 (Figure 8). These findings suggest that the augmented AKT phosphorylation that is observed in the presence of antioxidants, and, presumably its kinase activity, inhibits autophagy. We propose, therefore, that AKT is an important target for endogenous ROS and that a sustained inhibitory effect on AKT activity by physiological levels of endogenous ROS is necessary for the promotion of autophagy in skeletal muscle cells. This proposition is also based on numerous reports identifying AKT as a redox-sensitive kinase. Indeed, recent studies have revealed that ROS directly oxidize several cysteine residues of AKT, triggering the formation of intramolecular disulfide bonds and inactivation of AKT kinase activity (173). We should emphasize that the inhibitory effect of ROS on AKT appears to be a relatively less important mechanism in the case of EBSS-induced autophagy as compared to basal autophagy and autophagy induced by mTORC1 inhibition

(Figure 8). This implies that processes downstream from autophagosome initiation may also be targets through which endogenous ROS promote autophagy in skeletal muscles.

SECTION 6 – TABLES

TABLE 1: Primers used in real-time PCR experiments to detect expressions of autophagy-related genes and muscle-specific E3 ligases.

Gene			Accession #
Map1 (LC3B)	F	5'-CGATACAAGGGGGAGAAGCA-3'	NM_026160
	R	5'- ACTTCGGAGATGGGAGTGGA-3'	
Gabarapl1	F	5'- CATCGTGAGAAGGCTCCTA-3'	NM_020590
	R	5'- ATACAGCTGGCCCATGGTAG-3'	
Bnip3	F	5'-TTCCACTAGCACCTTCTGATGA-3'	NM_009760
	R	5'-GAACACCGCATTTACAGAACAA-3'	
Atrogin-1	F	5'- TGGGTGTATCGGATGGAGAC-3'	NM_026346
	R	5'- TCAGCCTCTGCATGATGTTC-3'	
MuRF1	F	5'-AGAAGCTGGGCTTCATCGAG-3'	NM_001039048
	R	5'- TGCTTGGCACTTGAGAGGAA-3'	
β-Actin	F	5'- CTGGCTCCTAGCACCATGAAGAT-3'	NM_007393
	R	5'- GGTGGACAGTGAGGCCAGGAT-3'	

SECTION 7 – FIGURES

FIGURE 1

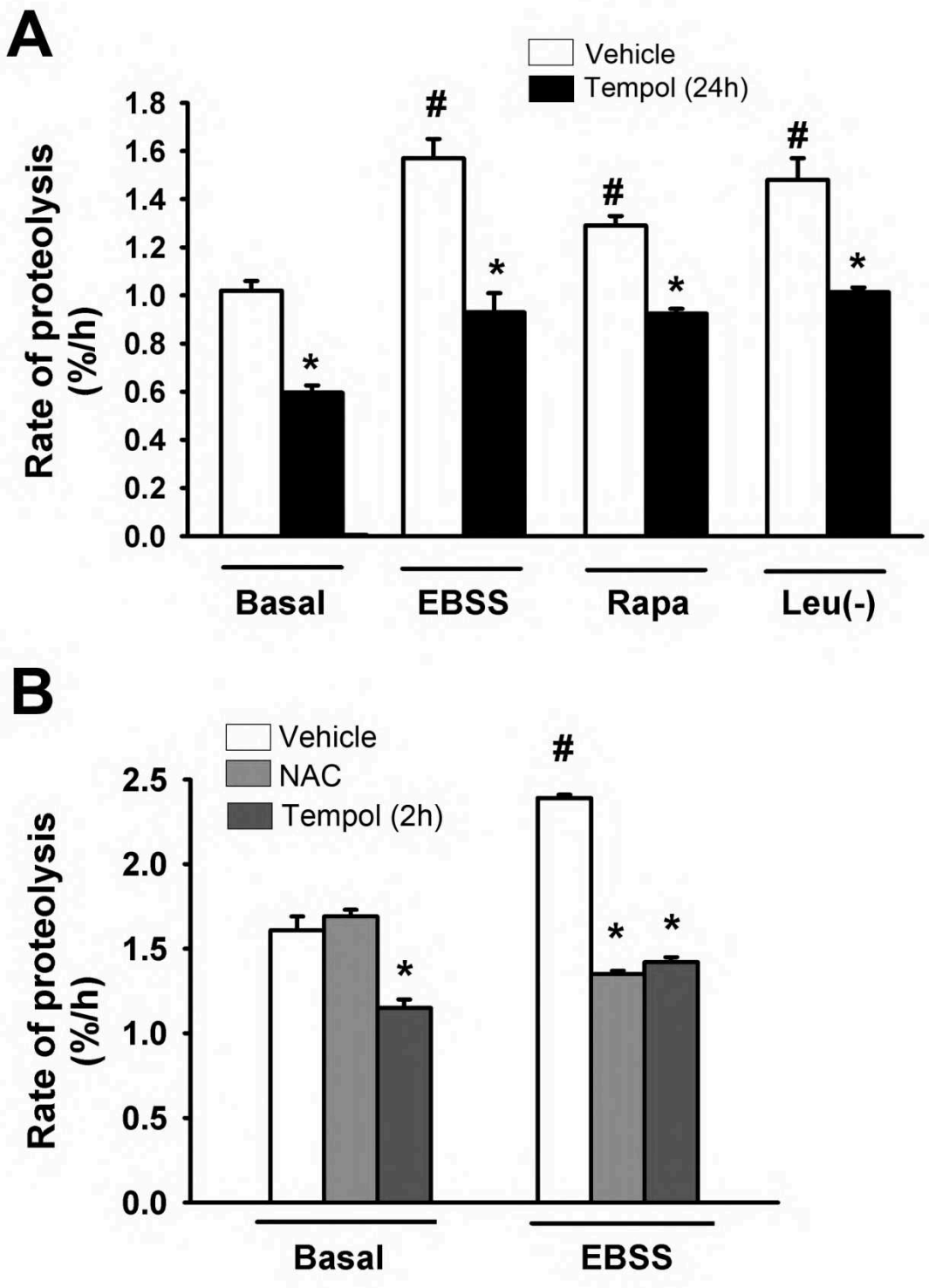

FIGURE 2

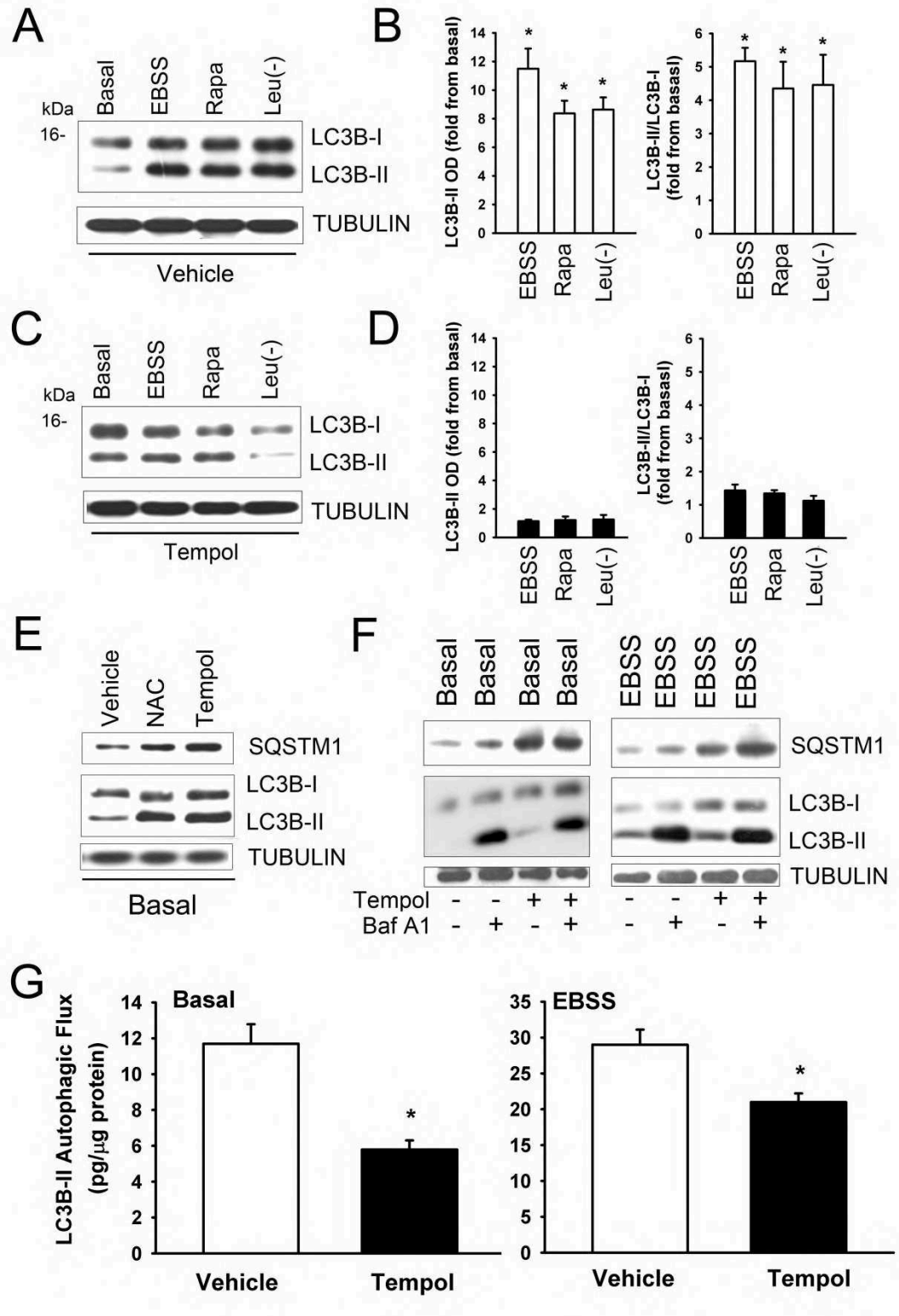
A
Basal
EBSS
Rapa
Leu(-)
kDa
16-
LC3B-I
LC3B-II
TUBULIN
Vehicle
B
LC3B-II OD (fold from basal)
LC3B-II/LC3B-I (fold from basasl)
EBSS
Rapa
Leu(-)
C
Tempol
D
E
Vehicle
NAC
Tempol
SQSTM1
Basal
F
Tempol
Baf A1
G
LC3B-II Autophagic Flux (pg/μg protein)
Basal
EBSS
Vehicle
Tempol

FIGURE 3

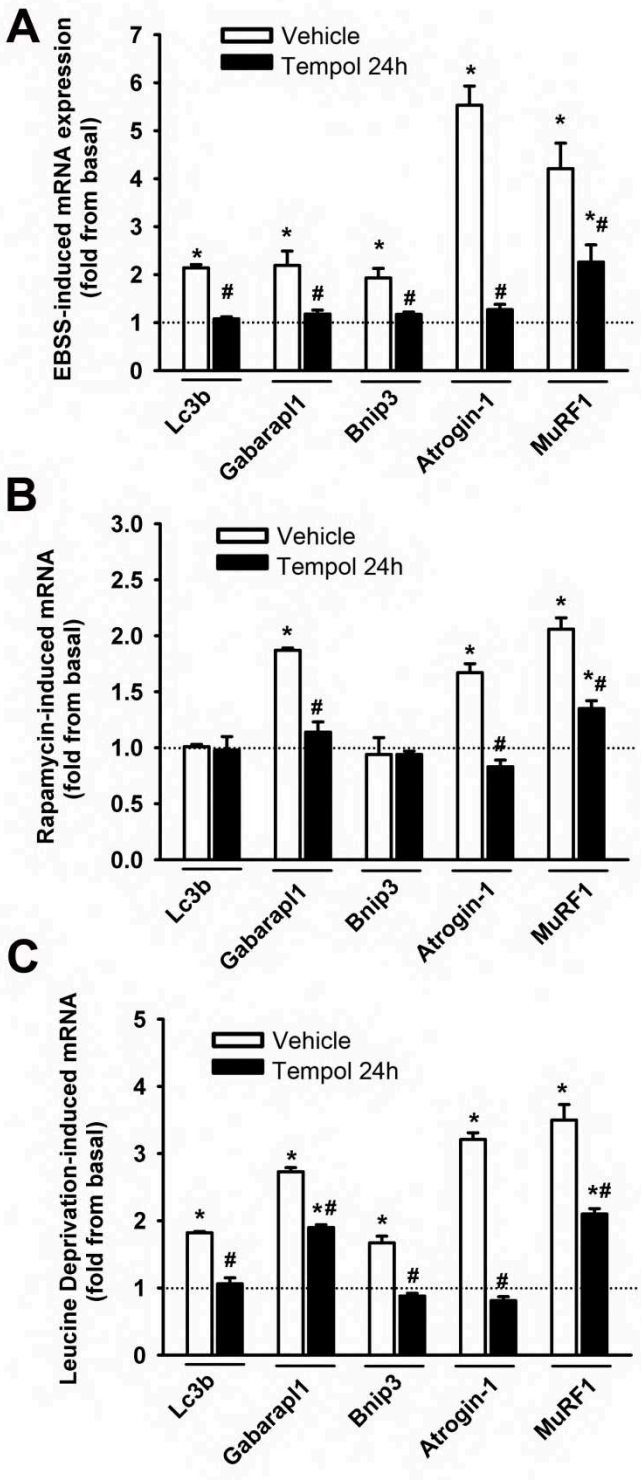
A
EBSS-induced mRNA expression (fold from basal)
Vehicle
Tempol 24h
Lc3b
Gabarapl1
Bnip3
Atrogin-1
MuRF1
B
Rapamycin-induced mRNA (fold from basal)
C
Leucine Deprivation-induced mRNA (fold from basal)

FIGURE 4

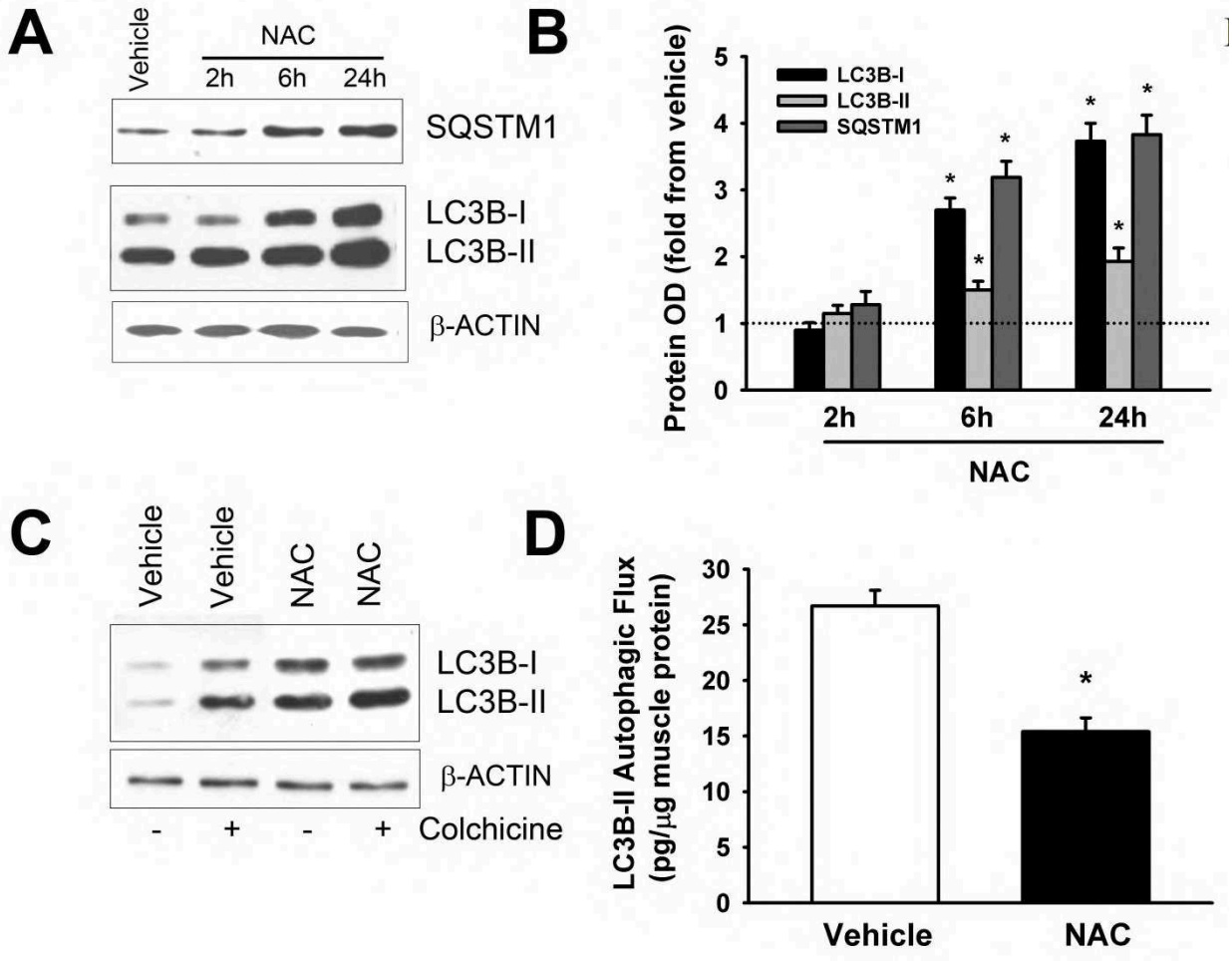
A
Vehicle
NAC
2h
6h
24h
SQSTM1
LC3B-I
LC3B-II
β-ACTIN
B
Protein OD (fold from vehicle)
LC3B-I
LC3B-II
SQSTM1
2h
6h
24h
NAC
C
Vehicle
Vehicle
NAC
NAC
LC3B-I
LC3B-II
β-ACTIN
- + - + Colchicine
D
LC3B-II Autophagic Flux
(pg/μg muscle protein)
Vehicle
NAC

FIGURE 5

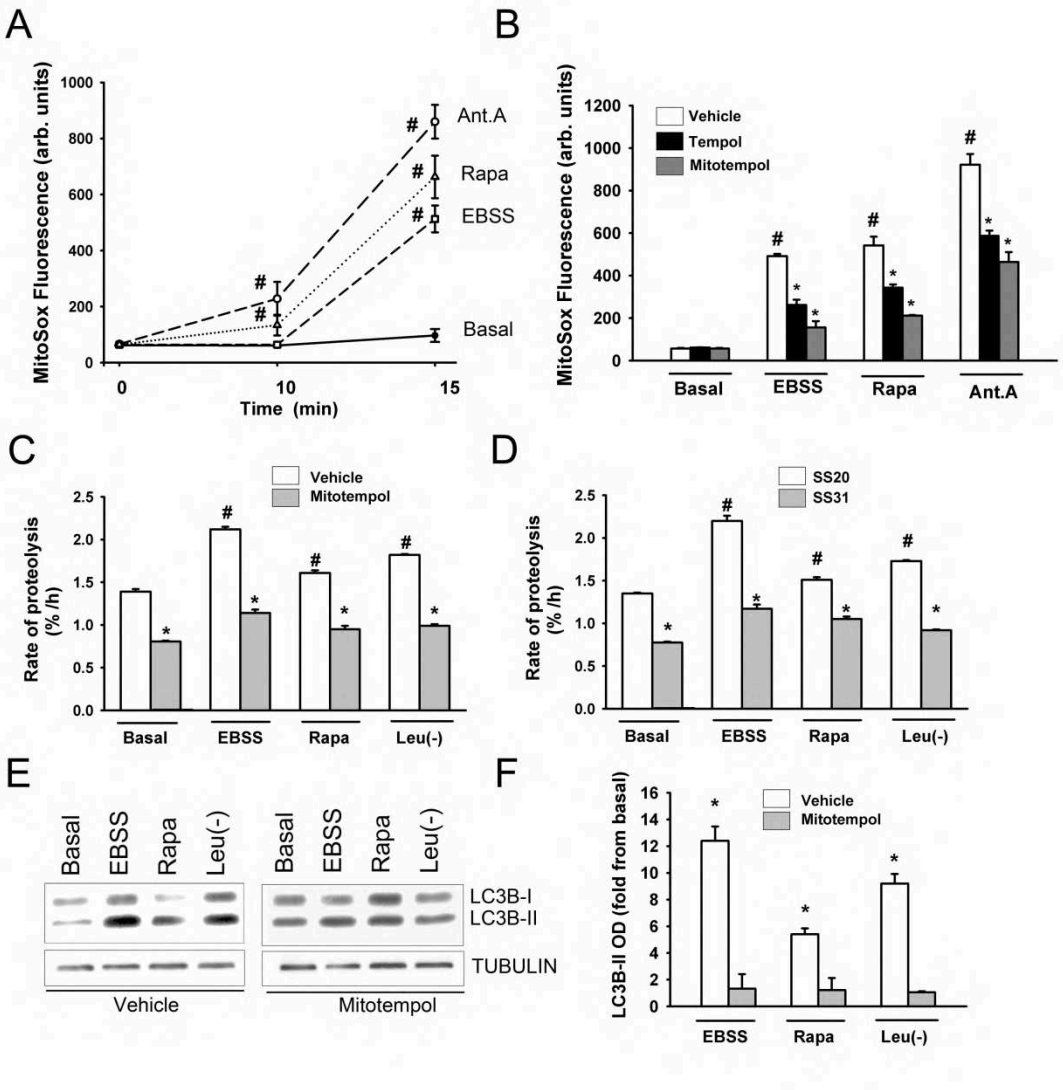
A
MitoSox Fluorescence (arb. units)
Time (min)
Ant.A
Rapa
EBSS
Basal
B
MitoSox Fluorescence (arb. units)
Vehicle
Tempol
Mitotempol
Basal
EBSS
Rapa
Ant.A
C
Rate of proteolysis (% /h)
Vehicle
Mitotempol
Basal
EBSS
Rapa
Leu(-)
D
Rate of proteolysis (% /h)
SS20
SS31
Basal
EBSS
Rapa
Leu(-)
E
Basal
EBSS
Rapa
Leu(-)
LC3B-I
LC3B-II
TUBULIN
Vehicle
Mitotempol
F
LC3B-II OD (fold from basal)
Vehicle
Mitotempol
EBSS
Rapa
Leu(-)

FIGURE 6

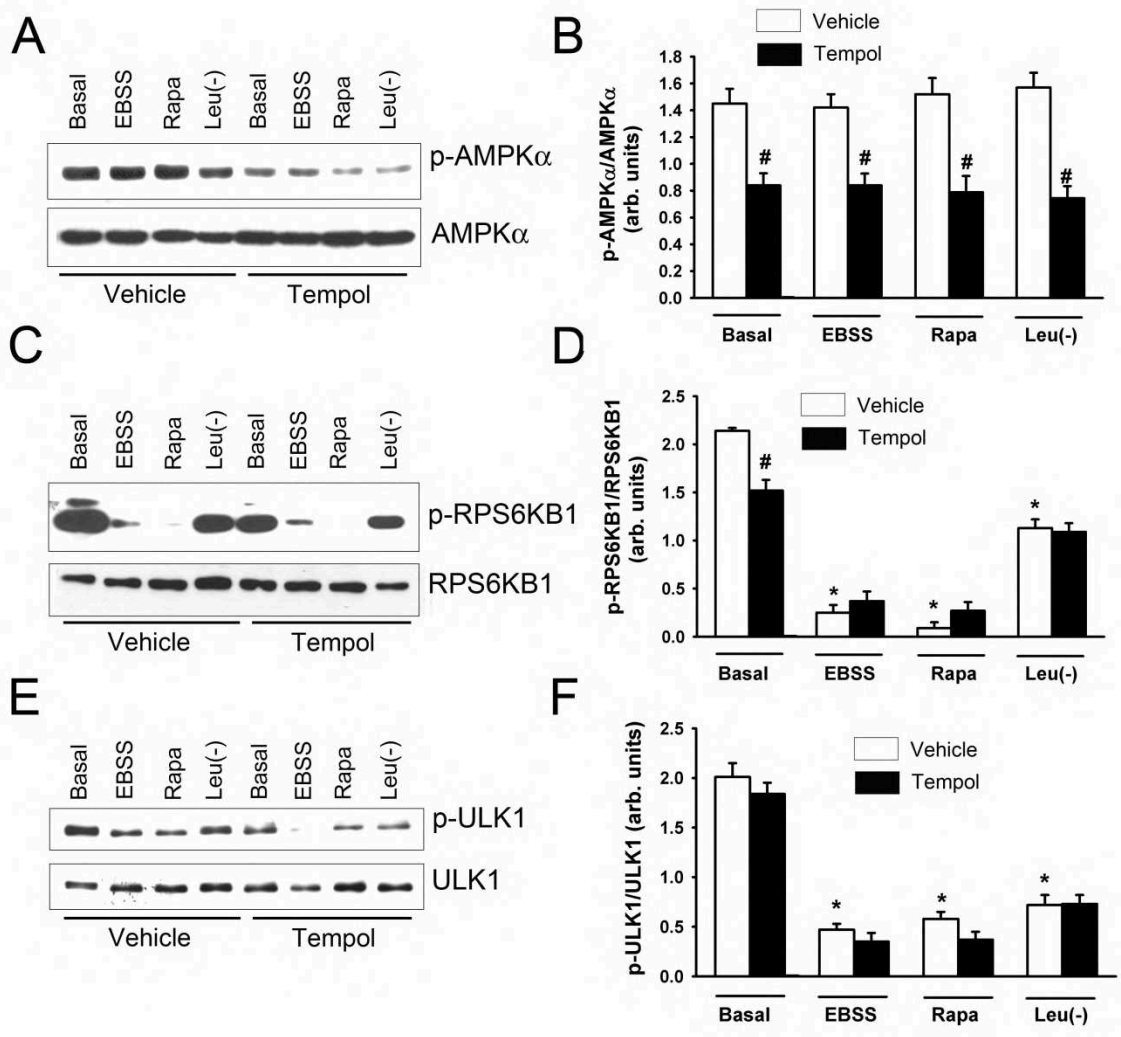
A
Basal
EBSS
Rapa
Leu(-)
Basal
EBSS
Rapa
Leu(-)
p-AMPKα
AMPKα
Vehicle
Tempol
B
Vehicle
Tempol
p-AMPKα/AMPKα (arb. units)
1.8
1.6
1.4
1.2
1.0
0.8
0.6
0.4
0.2
0.0
#
Basal
EBSS
Rapa
Leu(-)
C
p-RPS6KB1
RPS6KB1
D
p-RPS6KB1/RPS6KB1 (arb. units)
2.5
2.0
1.5
1.0
0.5
0.0
*
E
p-ULK1
ULK1
F
p-ULK1/ULK1 (arb. units)

FIGURE 7

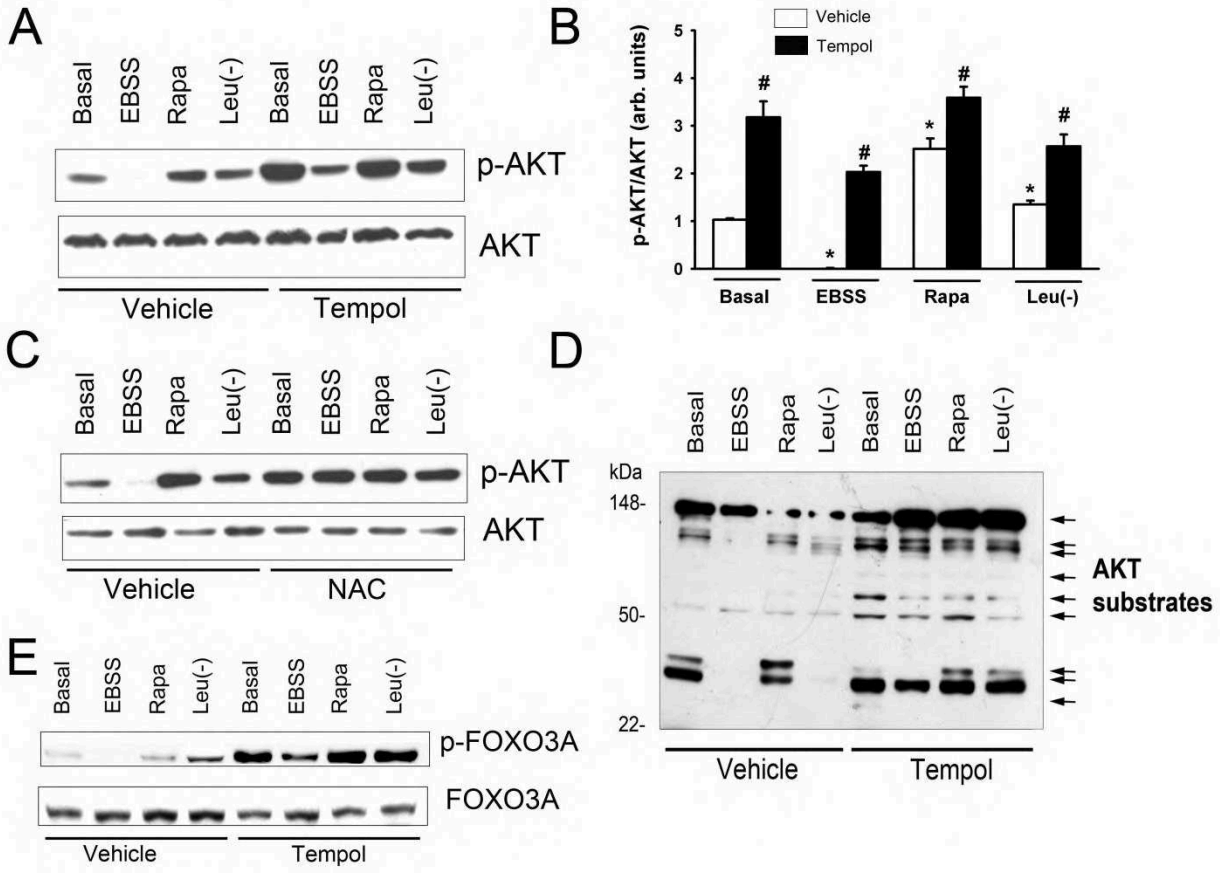
A
Basal
EBSS
Rapa
Leu(-)
Basal
EBSS
Rapa
Leu(-)
p-AKT
AKT
Vehicle
Tempol
B
Vehicle
Tempol
p-AKT/AKT (arb. units)
Basal
EBSS
Rapa
Leu(-)
C
p-AKT
AKT
Vehicle
NAC
D
kDa
148-
50-
22-
AKT substrates
Vehicle
Tempol
E
p-FOXO3A
FOXO3A
Vehicle
Tempol

FIGURE 8

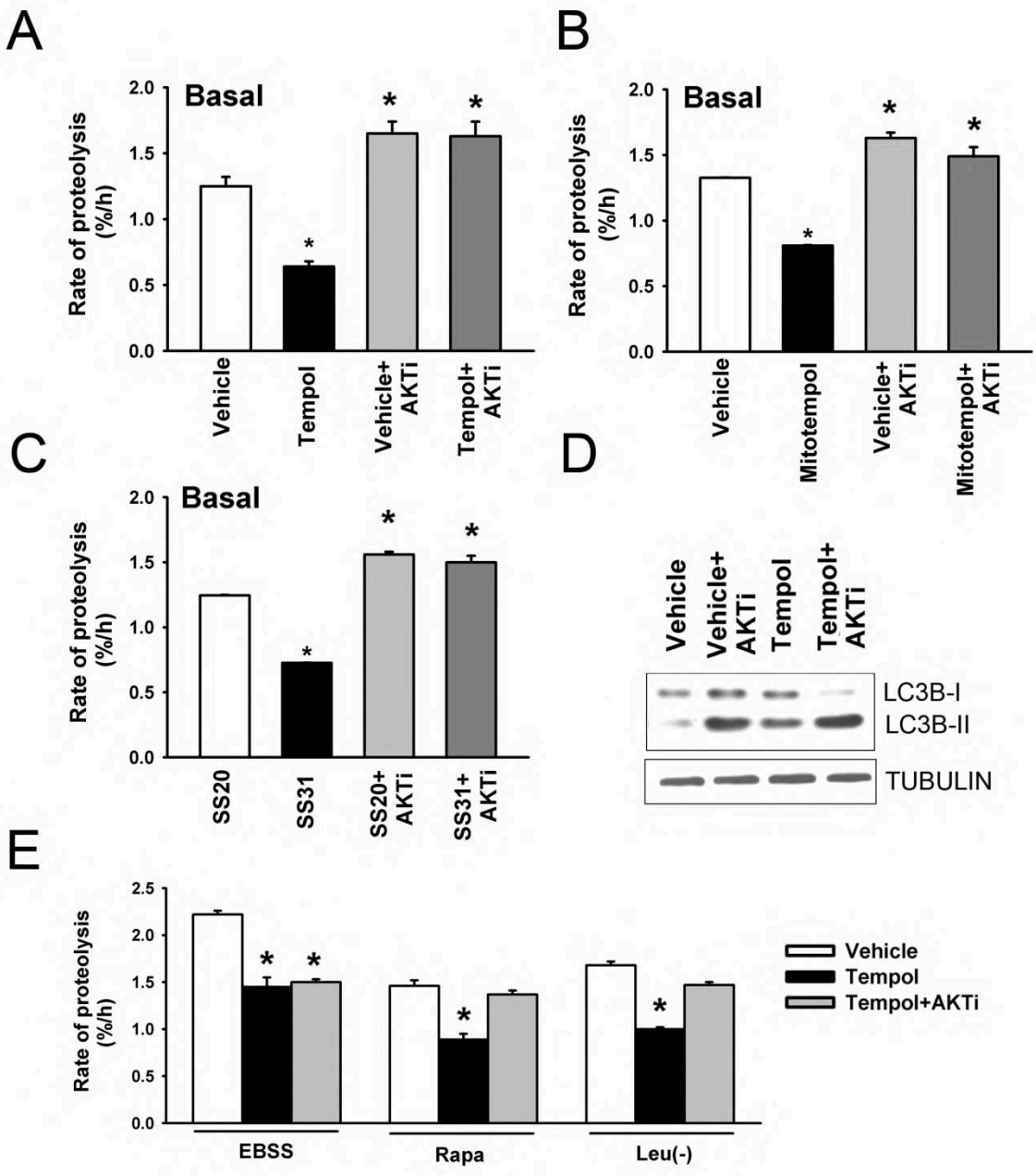
A
Basal
Rate of proteolysis (%/h)
2.0
1.5
1.0
0.5
0.0
Vehicle
Tempol
Vehicle+ AKTi
Tempol+ AKTi
B
Basal
Rate of proteolysis (%/h)
Vehicle
Mitotempol
Vehicle+ AKTi
Mitotempol+ AKTi
C
Basal
Rate of proteolysis (%/h)
SS20
SS31
SS20+ AKTi
SS31+ AKTi
D
Vehicle
Vehicle+ AKTi
Tempol
Tempol+ AKTi
LC3B-I
LC3B-II
TUBULIN
E
Rate of proteolysis (%/h)
2.5
2.0
1.5
1.0
0.5
0.0
EBSS
Rapa
Leu(-)
Vehicle
Tempol
Tempol+AKTi

SUPPLEMENTARY FIGURE 1

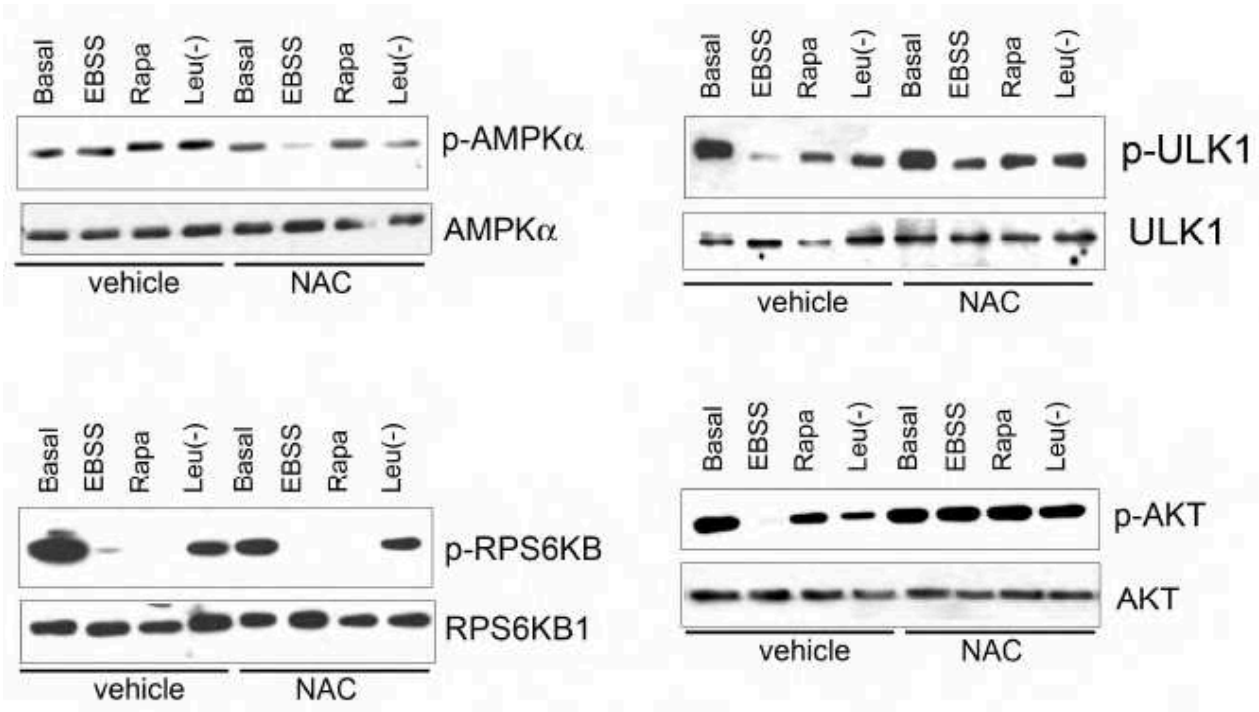

SUPPLEMENTARY FIGURE 2

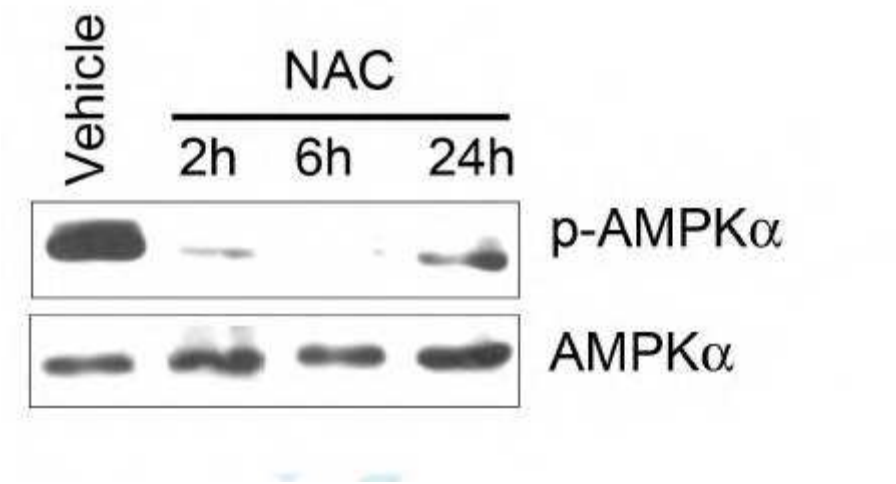

SUPPLEMENTARY FIGURE 3

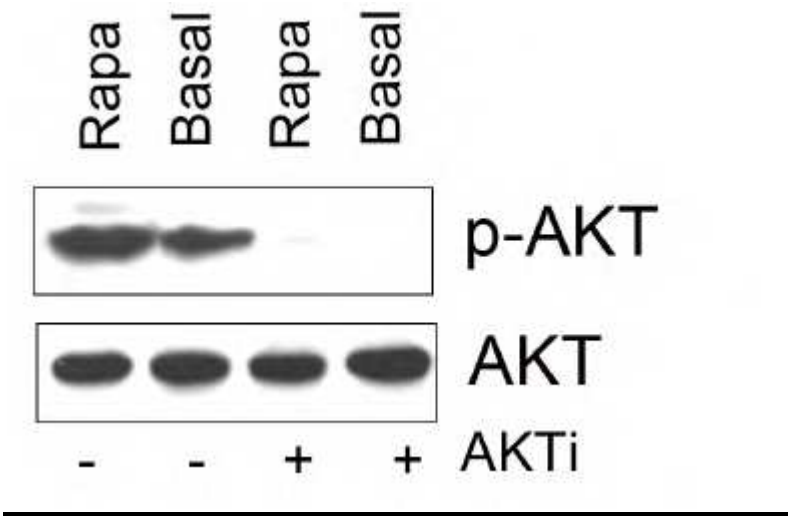

SECTION 8: FIGURE LEGENDS

Figure 1:

A: Rates of proteolysis in C2C12 myotubes pre-incubated for 24 hr in differentiation medium (DM) containing vehicle (PBS) or tempol (10 mM). Myotubes maintained in DM (basal conditions), EBSS medium, DM containing rapamycin (Rapa, 200 ng/ml), or DM lacking leucine (Leu(-)). Proteolysis measured over 4 hr. Values expressed as means ± SEM. $^{\#}P<0.05$ compared to basal conditions. *P<0.05 compared to vehicle.

B: Rates of proteolysis in differentiated C2C12 myotubes pre-incubated in DM containing vehicle (PBS) or N-acetyl cysteine (NAC, 20 mM) for 30 min or in DM containing tempol (10 mM) for 2 hr. Myotubes maintained in these media (basal conditions) or EBSS. Proteolysis measured over 4 hr. Values expressed as means ± SEM. $^{\#}P<0.05$ compared to basal conditions. *P<0.05 compared to vehicle.

Figure 2:

A, C: Representative immunoblots of LC3B protein detected in C2C12 myotubes pre-incubated for 24 hr in DM containing vehicle (PBS, panel A) or tempol (10 mM, panel C). Myotubes maintained in these media (basal condition) for 1.5h or in EBSS, DM containing rapamycin (Rapa), or DM lacking leucine (Leu(-)).

B, D: LC3B-II protein optical densities and LC3B-II/LC3B-I ratios (both expressed as fold change from basal values) in C2C12 myotubes pre-incubated for 24 hr in vehicle (panel B) or tempol (panel D) and maintained in EBSS medium, DM containing rapamycin (Rapa), or DM lacking leucine (Leu(-)). Values expressed as means ± SEM. *P<0.05 compared to basal values.

E: Representative immunoblots of SQSTM1 (p62), LC3B and TUBULIN in C2C12 myotubes pre-incubated for 24 hr in DM containing vehicle (PBS) or tempol or DM containing NAC for 2 hr. Note increases in SQSTM1, LC3B-I, and LC3B-II intensities in myotubes pre-incubated in NAC or tempol compared to vehicle.

F: Representative immunoblots of SQSTM1, LC3B, and TUBULIN in C2C12 myotubes pre-incubated for 24 hr in DM containing vehicle (PBS) or tempol. Myotubes maintained for 1.5 hr in DM containing1.5 ml of PBS or 200 nm of bafilomycin A1 (basal condition) or EBSS containing 1.5 ml of PBS or 200 nm of bafilomycin A1. Negative symbols indicate presence of PBS.

G: LC3B-II autophagic flux in C2C12 myotubes pre-incubated for 24 hr in DM containing vehicle or tempol. Myotubes maintained in these media or EBSS. Values expressed as means ± SEM. *P<0.05 compared to vehicle.

Figure 3: mRNA expressions of *Lc3b*, *Gabarapl1*, *Bnip3*, *Atrogin-1* and *MuRF1* in differentiated C2C12 myotubes pre-incubated for 24 hr in DM containing vehicle or tempol and maintained for an additional 1.5 hr in these media (basal condition), EBSS (panel A), DM containing rapamycin (panel B), DM lacking leucine (panel C). Values expressed as means ± SEM of fold change from basal values. *P<0.05 compared to basal condition. $^{\#}$P<0.05 compared to vehicle.

Figure 4:

A-B: Representative immunoblots and protein optical densities of SQSTM1 and LC3B-I and LC3B-II protein in diaphragms of mice injected with vehicle (PBS) or NAC (500 mg/kg).

Animals euthanized 2, 6 or 24 hr after PBS or NAC injection. Optical densities expressed as fold change from vehicle-treated animals (means ± SEM). *P<0.05 compared to vehicle.

C: Representative immunoblots of LC3B and b-ACTIN in diaphragms of mice injected with PBS or colchicine (0.4 mg/kg/day), followed by a second injection of PBS or NAC. Animals euthanized 24 hr after second injection.

D: LC3B-II autophagic flux in diaphragms of mice injected with vehicle or NAC. Values expressed as means ± SEM.*P<0.05 compared to vehicle.

Figure 5:

A: MitoSOX Red™ fluorescence in C2C12 myotubes incubated in HBSS buffer containing MitoSOX™ Red reagent (5 mM) for 30 min, washed of HBSS buffer then maintained in DM (basal condition), EBSS, or DM containing rapamycin (Rapa) or antimycin A (complex III inhibitor). Fluorescence measured immediately, 10, and 15 min after incubation in media. Values (arbitrary units) expressed as means ± SEM. #P<0.05 compared to basal values.

B: MitoSOX Red™ fluorescence in C2C12 myotubes pre-incubated in DM containing vehicle or tempol for 24 hr or in DM containing mito-tempol (500 mM) for 2 hr, washed of media then incubated in HBSS buffer containing MitoSOX™ Red reagent for 30 min. Myotubes then maintained for 15 min in DM (basal condition), EBSS, or DM containing rapamycin or antimycin A. Values (arbitrary units) expressed as means ± SEM. #P<0.05 compared to basal values. *P<0.05 compared to vehicle.

C: Rates of proteolysis in C2C12 myotubes pre-incubated for 2 hr in DM containing DMSO (vehicle) or mito-tempol (500 mM) then maintained in DM (basal condition), EBSS, or DM containing rapamycin or lacking leucine. Proteolysis measured over 4 hr. Values expressed as means ± SEM. $^{\#}P<0.05$ compared to basal values. *P<0.05 compared to vehicle.

D: Rates of proteolysis in C2C12 myotubes pre-incubated for 2 hr in DM containing SS20 (control peptide, 1 mM) or SS31 (inhibitor of mitochondrial ROS, 1 mM) then maintained in DM (basal condition), EBSS, or DM containing rapamycin or lacking leucine. Proteolysis measured over 4 hr. Values expressed as means ± SEM. $^{\#}P<0.05$ compared to basal values. *P<0.05 compared to vehicle.

E-F: Representative immunoblots of LC3B and LC3B-II optical densities of C2C12 myotubes pre-incubated for 2 hr in DM containing DMSO (vehicle) or mito-tempol then maintained for 1.5 hr in DM (basal condition), EBSS, or DM containing rapamycin or lacking leucine. Values expressed as means ± SEM.*P<0.05 compared to basal values.

Figure 6:

Representative immunoblots and phosphorylated to total protein ratios of AMPKα, RPS6KB1, and ULK1 in C2C12 myotubes pre-incubated for 24 hr in DM containing vehicle (PBS) or tempol then maintained for 1.5 hr in DM (basal condition), EBSS, or DM containing rapamycin or lacking leucine. Values expressed as means ± SEM. *P<0.05 compared to basal values. $^{\#}P<0.05$ compared to vehicle.

Figure 7:

A: Representative immunoblots and phosphorylated to total AKT protein ratios in C2C12 myotubes pre-incubated for 24 hr in DM containing vehicle (PBS) or tempol then maintained for 1.5 hr in DM (basal condition), EBSS, or DM containing rapamycin or lacking leucine. Values expressed as means ± SEM. *P<0.05 compared to basal values. $^{\#}$P<0.05 compared to vehicle.

C: Representative immunoblots of phosphorylated and total AKT protein ratios in C2C12 myotubes pre-incubated for 20 min in DM containing vehicle (PBS) or NAC then maintained for 1.5 hr in DM (basal condition), EBSS, or DM containing rapamycin or lacking leucine.

D, E: Representative immunoblots of phospho AKT substrates (panel D) and phosphorylated and total FOXO3A protein in C2C12 myotubes pre-incubated for 24 h in DM containing vehicle (PBS) or tempol then maintained for 1.5 hr in DM (basal condition), EBSS, or DM containing rapamycin or lacking leucine.

Figure 8:

A: Proteolysis rates in differentiated C2C12 myotubes pre-incubated for 24 hr in DM containing PBS (vehicle) or tempol then left untreated or treated with 20 mM triciribine (AKTi). Proteolysis measured over 4 hr. Values expressed as means ± SEM. *P<0.05 compared to vehicle in the absence of AKTi.

B: Proteolysis rates measured in differentiated C2C12 myotubes pre-incubated for 2 hr in DM containing DMSO (vehicle) or mito-tempol then left untreated or treated with AKTi. Proteolysis

measured over 4 hr. Values expressed as means ± SEM. *P<0.05 compared to vehicle in the absence of ATKi.

C: Proteolysis rates in differentiated C2C12 myotubes pre-incubated for 2 hr in DM containing SS20 or SS31 peptides then left untreated or treated with AKTi. Proteolysis measured over 4 hr. Values expressed as means ± SEM. *P<0.05 compared to SS20 in the absence of AKTi.

D: Representative immunoblots of LC3B and TUBULIN proteins in differentiated C2C12 myotubes pre-incubated for 24 hr in vehicle (PBS) or tempol then left untreated or treated with AKTi. Myotubes were collected 1.5 hr after treatment.

E: Proteolysis rates in differentiated C2C12 myotubes pre-incubated for 24h in DM containing PBS (vehicle) or tempol then maintained in DM, EBSS, or DM containing rapamycin or lacking leucine in the absence and presence of AKTi. Proteolysis measured over 4h. Values expressed as means ± SEM. *P<0.05 compared to vehicle in the absence of ATKi.

Supplementary Figure 1:

Representative immunoblots of phosphorylated and total AMPKα, RPS6K1 and ULK1 measured in C2C12 myotubes pre-incubated for 30 min with differentiation medium (DM) containing vehicle (PBS) or N-acetyl cysteine (NAC) and were then maintained for 1.5h in DM (basal condition), DM containing rapamycin, DM lacking leucine or maintained in EBSS buffer.

Supplementary Figure 2:

Regulation of the phosphorylated and total levels of AMPKα in the diaphragms of mice injected with vehicle (PBS) or NAC (500 mg/kg) i.p. and euthanized 2,6 and 24 hrs later.

Supplementary Figure 3:

Verification of efficiency of triciribine (AKTi) in inhibiting AKT phosphorylation in C2C12 myotubes. These cells were maintained in differentiation medium (DM) containing PBS (vehicle, negative sign) or AKTi (20μM) in the absence and presence of rapamycin (Rapa, 200ng/ml).

SECTION 9: Reference List

1. **Arthur PG, Grounds MD and Shavlakadze T**. Oxidative stress as a therapeutic target during muscle wasting: considering the complex interactions. *Curr Opin Clin Nutr Metab Care* 11: 408-416, 2008.

2. **Aruoma OI, Halliwell B, Hoey BM and Butler J**. The antioxidant action of N-acetylcysteine: its reaction with hydrogen peroxide, hydroxyl radical, superoxide, and hypochlorous acid. *Free Radic Biol Med* 6: 593-597, 1989.

3. **Atlashkin V, Kreykenbohm V, Eskelinen EL, Wenzel D, Fayyazi A and Fischer von MG**. Deletion of the SNARE vti1b in mice results in the loss of a single SNARE partner, syntaxin 8. *Mol Cell Biol* 23: 5198-5207, 2003.

4. **Aucello M, Dobrowolny G and Musaro A**. Localized accumulation of oxidative stress causes muscle atrophy through activation of an autophagic pathway. *Autophagy* 5: 527-529, 2009.

5. **Axe EL, Walker SA, Manifava M, Chandra P, Roderick HL, Habermann A, Griffiths G and Ktistakis NT**. Autophagosome formation from membrane compartments enriched in phosphatidylinositol 3-phosphate and dynamically connected to the endoplasmic reticulum. *J Cell Biol* 182: 685-701, 2008.

6. **Azad MB, Chen Y and Gibson SB**. Regulation of autophagy by reactive oxygen species (ROS): implications for cancer progression and treatment. *Antioxid Redox Signal* 11: 777-790, 2009.

7. **Balaban RS, Nemoto S and Finkel T**. Mitochondria, oxidants, and aging. *Cell* 120: 483-495, 2005.

8. **Barbieri E and Sestili P**. Reactive oxygen species in skeletal muscle signaling. *J Signal Transduct* 2012: 982794, 2012.

9. **Barreiro E and Hussain SN**. Protein carbonylation in skeletal muscles: impact on function. *Antioxid Redox Signal* 12: 417-429, 2010.

10. **Bejarano E and Cuervo AM**. Chaperone-mediated autophagy. *Proc Am Thorac Soc* 7: 29-39, 2010.

11. **Bernardi P and Bonaldo P**. Dysfunction of mitochondria and sarcoplasmic reticulum in the pathogenesis of collagen VI muscular dystrophies. *Ann N Y Acad Sci* 1147: 303-311, 2008.

12. **Black CD, Samuni A, Cook JA, Krishna CM, Kaufman DC, Malech HL and Russo A**. Kinetics of superoxide production by stimulated neutrophils. *Arch Biochem Biophys* 286: 126-131, 1991.

13. **Bloom DA and Jaiswal AK**. Phosphorylation of Nrf2 at Ser40 by protein kinase C in response to antioxidants leads to the release of Nrf2 from INrf2, but is not required for Nrf2 stabilization/accumulation in the nucleus and transcriptional activation of antioxidant response element-mediated NAD(P)H:quinone oxidoreductase-1 gene expression. *J Biol Chem* 278: 44675-44682, 2003.

14. **Boczkowski J, Lisdero CL, Lanone S, Samb A, Carreras MC, Boveris A, Aubier M and Poderoso J**. Endogenous peroxynitrite mediates mitochondrial dysfunction in rat diaphragm during endotoxemia. *FASEB J* 13: 1637-1647, 1999.

15. **Bodine SC, Latres E, Baumhueter S, Lai VK, Nunez L, Clarke BA, Poueymirou WT, Panaro FJ, Na E, Dharmarajan K, Pan ZQ, Valenzuela DM, DeChiara TM, Stitt TN, Yancopoulos GD and Glass DJ**. Identification of ubiquitin ligases required for skeletal muscle atrophy. *Science* 294: 1704-1708, 2001.

16. **Bodine SC, Stitt TN, Gonzalez M, Kline WO, Stover GL, Bauerlein R, Zlotchenko E, Scrimgeour A, Lawrence JC, Glass DJ and Yancopoulos GD**. Akt/mTOR pathway is a crucial regulator of skeletal muscle hypertrophy and can prevent muscle atrophy in vivo. *Nat Cell Biol* 3: 1014-1019, 2001.

17. **Brocca L, Cannavino J, Coletto L, Biolo G, Sandri M, Bottinelli R and Pellegrino MA**. The time course of the adaptations of human muscle proteome to bed rest and the underlying mechanisms. *J Physiol* 590: 5211-5230, 2012.

18. **Brunet A, Bonni A, Zigmond MJ, Lin MZ, Juo P, Hu LS, Anderson MJ, Arden KC, Blenis J and Greenberg ME**. Akt promotes cell survival by phosphorylating and inhibits a forkhead transcription factor. *Cell* 96: 857-868, 1999.

19. **Cafe C, Testa MP, Sheldon PJ, French WP, Ellerby LM and Bredesen DE**. Loss of oxidation-reduction specificity in amyotrophic lateral sclerosis-associated CuZnSOD mutants. *J Mol Neurosci* 15: 71-83, 2000.

20. **Cantley LC**. The phosphoinositide 3-kinase pathway. *Science* 296: 1655-1657, 2002.

21. **Carmignac V, Svensson M, Korner Z, Elowsson L, Matsumura C, Gawlik KI, Allamand V and Durbeej M**. Autophagy is increased in laminin alpha2 chain-deficient muscle and its inhibition improves muscle morphology in a mouse model of MDC1A. *Hum Mol Genet* 20: 4891-4902, 2011.

22. **Chang NC, Nguyen M, Bourdon J, Risse PA, Martin J, Danialou G, Rizzuto R, Petrof BJ and Shore GC**. Bcl-2-associated autophagy regulator Naf-1 required for maintenance of skeletal muscle. *Hum Mol Genet* 21: 2277-2287, 2012.

23. **Chen Y, Azad MB and Gibson SB**. Superoxide is the major reactive oxygen species regulating autophagy. *Cell Death Differ* 16: 1040-1052, 2009.

24. **Chen Y, McMillan-Ward E, Kong J, Israels SJ and Gibson SB**. Mitochondrial electron-transport-chain inhibitors of complexes I and II induce autophagic cell death mediated by reactive oxygen species. *J Cell Sci* 120: 4155-4166, 2007.

25. **Clarke BA, Drujan D, Willis MS, Murphy LO, Corpina RA, Burova E, Rakhilin SV, Stitt TN, Patterson C, Latres E and Glass DJ**. The E3 Ligase MuRF1 degrades myosin heavy chain protein in dexamethasone-treated skeletal muscle. *Cell Metab* 6: 376-385, 2007.

26. **Cohen S, Brault JJ, Gygi SP, Glass DJ, Valenzuela DM, Gartner C, Latres E and Goldberg AL**. During muscle atrophy, thick, but not thin, filament components are degraded by MuRF1-dependent ubiquitylation. *J Cell Biol* 185: 1083-1095, 2009.

27. **Coirault C, Guellich A, Barbry T, Samuel JL, Riou B and Lecarpentier Y**. Oxidative stress of myosin contributes to skeletal muscle dysfunction in rats with chronic heart failure. *Am J Physiol Heart Circ Physiol* 292: H1009-H1017, 2007.

28. **Combaret L, Adegoke OA, Bedard N, Baracos V, Attaix D and Wing SS**. USP19 is a ubiquitin-specific protease regulated in rat skeletal muscle during catabolic states. *Am J Physiol Endocrinol Metab* 288: E693-E700, 2005.

29. **Cong H, Sun L, Liu C and Tien P**. Inhibition of atrogin-1/MAFbx expression by adenovirus-delivered small hairpin RNAs attenuates muscle atrophy in fasting mice. *Hum Gene Ther* 22: 313-324, 2011.

30. **Cuschieri J and Maier RV**. Mitogen-activated protein kinase (MAPK). *Crit Care Med* 33: S417-S419, 2005.

31. **de DC, PRESSMAN BC, GIANETTO R, Wattiaux R and APPELMANS F**. Tissue fractionation studies. 6. Intracellular distribution patterns of enzymes in rat-liver tissue. *Biochem J* 60: 604-617, 1955.

32. **De JB, Sharshar T, Hopkinson N and Outin H**. Paresis following mechanical ventilation. *Curr Opin Crit Care* 10: 47-52, 2004.

33. **Debigare R, Cote CH and Maltais F**. Peripheral muscle wasting in chronic obstructive pulmonary disease. Clinical relevance and mechanisms. *Am J Respir Crit Care Med* 164: 1712-1717, 2001.

34. **Derde S, Hermans G, Derese I, Guiza F, Hedstrom Y, Wouters PJ, Bruyninckx F, D'Hoore A, Larsson L, Van den BG and Vanhorebeek I**. Muscle atrophy and preferential loss of myosin in prolonged critically ill patients*. *Crit Care Med* 40: 79-89, 2012.

35. **Deval C, Mordier S, Obled C, Bechet D, Combaret L, Attaix D and Ferrara M**. Identification of cathepsin L as a differentially expressed message associated with skeletal muscle wasting. *Biochem J* 360: 143-150, 2001.

36. **Djavaheri-Mergny M, Amelotti M, Mathieu J, Besancon F, Bauvy C, Souquere S, Pierron G and Codogno P**. NF-kappaB activation represses tumor necrosis factor-alpha-induced autophagy. *J Biol Chem* 281: 30373-30382, 2006.

37. **Dobrowolny G, Aucello M, Rizzuto E, Beccafico S, Mammucari C, Boncompagni S, Belia S, Wannenes F, Nicoletti C, Del PZ, Rosenthal N, Molinaro M, Protasi F, Fano G, Sandri M and Musaro A**. Skeletal muscle is a primary target of SOD1G93A-mediated toxicity. *Cell Metab* 8: 425-436, 2008.

38. **Egan DF, Shackelford DB, Mihaylova MM, Gelino S, Kohnz RA, Mair W, Vasquez DS, Joshi A, Gwinn DM, Taylor R, Asara JM, Fitzpatrick J, Dillin A, Viollet B, Kundu M, Hansen M and Shaw RJ**. Phosphorylation of ULK1 (hATG1) by AMP-activated protein kinase connects energy sensing to mitophagy. *Science* 331: 456-461, 2011.

39. **Emerling BM, Weinberg F, Snyder C, Burgess Z, Mutlu GM, Viollet B, Budinger GR and Chandel NS**. Hypoxic activation of AMPK is dependent on mitochondrial ROS but independent of an increase in AMP/ATP ratio. *Free Radic Biol Med* 46: 1386-1391, 2009.

40. **Fimia GM, Stoykova A, Romagnoli A, Giunta L, Di BS, Nardacci R, Corazzari M, Fuoco C, Ucar A, Schwartz P, Gruss P, Piacentini M, Chowdhury K and Cecconi F**. Ambra1 regulates autophagy and development of the nervous system. *Nature* 447: 1121-1125, 2007.

41. **Fujita J, Tsujinaka T, Yano M, Ebisui C, Saito H, Katsume A, Akamatsu K, Ohsugi Y, Shiozaki H and Monden M**. Anti-interleukin-6 receptor antibody prevents muscle atrophy in colon-26 adenocarcinoma-bearing mice with modulation of lysosomal and ATP-ubiquitin-dependent proteolytic pathways. *Int J Cancer* 68: 637-643, 1996.

42. **Funderburk SF, Wang QJ and Yue Z**. The Beclin 1-VPS34 complex--at the crossroads of autophagy and beyond. *Trends Cell Biol* 20: 355-362, 2010.

43. **Ganley IG, Lam dH, Wang J, Ding X, Chen S and Jiang X**. ULK1.ATG13.FIP200 complex mediates mTOR signaling and is essential for autophagy. *J Biol Chem* 284: 12297-12305, 2009.

44. **Ganley IG, Lam dH, Wang J, Ding X, Chen S and Jiang X**. ULK1-ÀATG13-ÀFIP200 Complex Mediates mTOR Signaling and Is Essential for Autophagy. *Journal of Biological Chemistry* 284: 12297-12305, 2009.

45. **Glickman MH and Ciechanover A**. The ubiquitin-proteasome proteolytic pathway: destruction for the sake of construction. *Physiol Rev* 82: 373-428, 2002.

46. **Gomes MD, Lecker SH, Jagoe RT, Navon A and Goldberg AL**. Atrogin-1, a muscle-specific F-box protein highly expressed during muscle atrophy. *Proc Natl Acad Sci U S A* 98: 14440-14445, 2001.

47. **Gomez-Cabrera MC, Domenech E and Vina J**. Moderate exercise is an antioxidant: upregulation of antioxidant genes by training. *Free Radic Biol Med* 44: 126-131, 2008.

48. **Grumati P, Coletto L, Sabatelli P, Cescon M, Angelin A, Bertaggia E, Blaauw B, Urciuolo A, Tiepolo T, Merlini L, Maraldi NM, Bernardi P, Sandri M and Bonaldo P**. Autophagy is defective in collagen VI muscular dystrophies, and its reactivation rescues myofiber degeneration. *Nat Med* 16: 1313-1320, 2010.

49. **Guo Z, Kozlov S, Lavin MF, Person MD and Paull TT**. ATM activation by oxidative stress. *Science* 330: 517-521, 2010.

50. **Gutierrez MG, Munafo DB, Beron W and Colombo MI**. Rab7 is required for the normal progression of the autophagic pathway in mammalian cells. *J Cell Sci* 117: 2687-2697, 2004.

51. **Gutteridge JM and Halliwell B**. Free radicals and antioxidants in the year 2000. A historical look to the future. *Ann N Y Acad Sci* 899: 136-147, 2000.

52. **Gutteridge JM and Halliwell B**. Free radicals and antioxidants in the year 2000. A historical look to the future. *Ann N Y Acad Sci* 899: 136-147, 2000.

53. **Hailey DW, Rambold AS, Satpute-Krishnan P, Mitra K, Sougrat R, Kim PK and Lippincott-Schwartz J**. Mitochondria supply membranes for autophagosome biogenesis during starvation. *Cell* 141: 656-667, 2010.

54. **Hall A, Karplus PA and Poole LB**. Typical 2-Cys peroxiredoxins--structures, mechanisms and functions. *FEBS J* 276: 2469-2477, 2009.

55. **Hamanaka RB and Chandel NS**. Mitochondrial reactive oxygen species regulate cellular signaling and dictate biological outcomes. *trends biochem sci* 35: 505-513, 2010.

56. **Handayaningsih AE, Iguchi G, Fukuoka H, Nishizawa H, Takahashi M, Yamamoto M, Herningtyas EH, Okimura Y, Kaji H, Chihara K, Seino S and Takahashi Y**. Reactive oxygen species play an essential role in IGF-I signaling and IGF-I-induced myocyte hypertrophy in C2C12 myocytes. *Endocrinology* 152: 912-921, 2011.

57. **Hanna RA, Quinsay MN, Orogo AM, Giang K, Rikka S and Gustafsson AB**. Microtubule-associated Protein 1 Light Chain 3 (LC3) Interacts with Bnip3 Protein to Selectively Remove Endoplasmic Reticulum and Mitochondria via Autophagy. *J Biol Chem* 287: 19094-19104, 2012.

58. **Hara T, Takamura A, Kishi C, Iemura S, Natsume T, Guan JL and Mizushima N**. FIP200, a ULK-interacting protein, is required for autophagosome formation in mammalian cells

1. *J Cell Biol* 181: 497-510, 2008.

59. **Haspel J, Shaik RS, Ifedigbo E, Nakahira K, Dolinay T, Englert JA and Choi AM**. Characterization of macroautophagic flux in vivo using a leupeptin-based assay. *Autophagy* 7: 629-642, 2011.

60. **Haycock JW, Jone P, Harris JB and Mantle D**. Differential susceptibility of human skeletal muscle proteins to free radical induced oxidative damage: a histochemical, immunocytochemical and electron microscopy study in vitro. *Acta Neuropath* 92: 331-340, 1996.

61. **Hosokawa N, Hara T, Kaizuka T, Kishi C, Takamura A, Miura Y, Iemura S, Natsume T, Takehana K, Yamada N, Guan JL, Oshiro N and Mizushima N**. Nutrient-dependent mTORC1 association with the ULK1-Atg13-FIP200 complex required for autophagy. *Mol Biol Cell* 20: 1981-1991, 2009.

62. **Hudlicka O, Brown M and Egginton S**. Angiogenesis in skeletal and cardiac muscle

27. *Physiol Rev* 72: 369-417, 1992.

63. **Itakura E, Kishi C, Inoue K and Mizushima N**. Beclin 1 forms two distinct phosphatidylinositol 3-kinase complexes with mammalian Atg14 and UVRAG. *Mol Biol Cell* 19: 5360-5372, 2008.

64. **Jackman RW and Kandarian SC**. The molecular basis of skeletal muscle atrophy. *Am J Physiol Cell Physiol* 287: C834-C843, 2004.

65. **Jansen JKS and Fladby T**. The perinatal reorganization of the innervation of skeletal muscle in mammals. *Progress in Neurobiology* 34: 39-90, 1990.

66. **Janssen-Heininger YM, Mossman BT, Heintz NH, Forman HJ, Kalyanaraman B, Finkel T, Stamler JS, Rhee SG and van d, V**. Redox-based regulation of signal transduction: principles, pitfalls, and promises. *Free Radic Biol Med* 45: 1-17, 2008.

67. **Jung CH, Jun CB, Ro SH, Kim YM, Otto NM, Cao J, Kundu M and Kim DH**. ULK-Atg13-FIP200 complexes mediate mTOR signaling to the autophagy machinery. *Mol Biol Cell* 20: 1992-2003, 2009.

68. **Kamata H, Honda S, Maeda S, Chang L, Hirata H and Karin M**. Reactive oxygen species promote TNFalpha-induced death and sustained JNK activation by inhibiting MAP kinase phosphatases. *Cell* 120: 649-661, 2005.

69. **Kamei Y, Miura S, Suzuki M, Kai Y, Mizukami J, Taniguchi T, Mochida K, Hata T, Matsuda J, Aburatani H, Nishino I and Ezaki O**. Skeletal muscle FOXO1 (FKHR) transgenic mice have less skeletal muscle mass, down-regulated Type I (slow twitch/red muscle) fiber genes, and impaired glycemic control. *J Biol Chem* 279: 41114-41123, 2004.

70. **Kaushik S and Cuervo AM**. Chaperone-mediated autophagy. *Methods Mol Biol* 445: 227-244, 2008.

71. **Kedar V, McDonough H, Arya R, Li HH, Rockman HA and Patterson C**. Muscle-specific RING finger 1 is a bona fide ubiquitin ligase that degrades cardiac troponin I. *Proc Natl Acad Sci U S A* 101: 18135-18140, 2004.

72. **Kelley MR, Georgiadis MM and Fishel ML**. APE1/Ref-1 role in redox signaling: translational applications of targeting the redox function of the DNA repair/redox protein APE1/Ref-1. *Curr Mol Pharmacol* 5: 36-53, 2012.

73. **Kiffin R, Bandyopadhyay U and Cuervo AM**. Oxidative stress and autophagy. *Antioxid Redox Signal* 8: 152-162, 2006.

74. **Kihara A, Kabeya Y, Ohsumi Y and Yoshimori T**. Beclin-phosphatidylinositol 3-kinase complex functions at the trans-Golgi network. *EMBO Rep* 2: 330-335, 2001.

75. **Kim DH, Sarbassov DD, Ali SM, King JE, Latek RR, Erdjument-Bromage H, Tempst P and Sabatini DM**. mTOR interacts with raptor to form a nutrient-sensitive complex that signals to the cell growth machinery. *Cell* 110: 163-175, 2002.

76. **Kim I, Rodriguez-Enriquez S and Lemasters JJ**. Selective degradation of mitochondria by mitophagy. *Arch Biochem Biophys* 462: 245-253, 2007.

77. **Kim J, Kundu M, Viollet B and Guan KL**. AMPK and mTOR regulate autophagy through direct phosphorylation of Ulk1. *Nat Cell Biol* 13: 132-141, 2011.

78. **Kim PK, Hailey DW, Mullen RT and Lippincott-Schwartz J**. Ubiquitin signals autophagic degradation of cytosolic proteins and peroxisomes. *Proc Natl Acad Sci U S A* 105: 20567-20574, 2008.

79. **Kirkland RA, Saavedra GM and Franklin JL**. Rapid activation of antioxidant defenses by nerve growth factor suppresses reactive oxygen species during neuronal apoptosis: evidence for a role in cytochrome c redistribution. *J Neurosci* 27: 11315-11326, 2007.

80. **Klionsky DJ**. Autophagy. *Curr Biol* 15: R282-R283, 2005.

81. **Klionsky DJ, Abeliovich H, Agostinis P, Agrawal DK, Aliev G, Askew DS, Baba M, Baehrecke EH, Bahr BA, Ballabio A, Bamber BA, Bassham DC, Bergamini E, Bi X, Biard-Piechaczyk M, Blum JS, Bredesen DE, Brodsky JL, Brumell JH, Brunk UT, Bursch W, Camougrand N, Cebollero E, Cecconi F, Chen Y, Chin LS, Choi A, Chu CT, Chung J, Clarke PG, Clark RS, Clarke SG, Clave C, Cleveland JL, Codogno P, Colombo MI, Coto-Montes A, Cregg JM, Cuervo AM, Debnath J,**

Demarchi F, Dennis PB, Dennis PA, Deretic V, Devenish RJ, Di SF, Dice JF, Difiglia M, nesh-Kumar S, Distelhorst CW, Djavaheri-Mergny M, Dorsey FC, Droge W, Dron M, Dunn WA, Jr., Duszenko M, Eissa NT, Elazar Z, Esclatine A, Eskelinen EL, Fesus L, Finley KD, Fuentes JM, Fueyo J, Fujisaki K, Galliot B, Gao FB, Gewirtz DA, Gibson SB, Gohla A, Goldberg AL, Gonzalez R, Gonzalez-Estevez C, Gorski S, Gottlieb RA, Haussinger D, He YW, Heidenreich K, Hill JA, Hoyer-Hansen M, Hu X, Huang WP, Iwasaki A, Jaattela M, Jackson WT, Jiang X, Jin S, Johansen T, Jung JU, Kadowaki M, Kang C, Kelekar A, Kessel DH, Kiel JA, Kim HP, Kimchi A, Kinsella TJ, Kiselyov K, Kitamoto K, Knecht E, Komatsu M, Kominami E, Kondo S, Kovacs AL, Kroemer G, Kuan CY, Kumar R, Kundu M, Landry J, Laporte M, Le W, Lei HY, Lenardo MJ, Levine B, Lieberman A, Lim KL, Lin FC, Liou W, Liu LF, Lopez-Berestein G, Lopez-Otin C, Lu B, Macleod KF, Malorni W, Martinet W, Matsuoka K, Mautner J, Meijer AJ, Melendez A, Michels P, Miotto G, Mistiaen WP, Mizushima N, Mograbi B, Monastyrska I, Moore MN, Moreira PI, Moriyasu Y, Motyl T, Munz C, Murphy LO, Naqvi NI, Neufeld TP, Nishino I, Nixon RA, Noda T, Nurnberg B, Ogawa M, Oleinick NL, Olsen LJ, Ozpolat B, Paglin S, Palmer GE, Papassideri I, Parkes M, Perlmutter DH, Perry G, Piacentini M, Pinkas-Kramarski R, Prescott M, Proikas-Cezanne T, Raben N, Rami A, Reggiori F, Rohrer B, Rubinsztein DC, Ryan KM, Sadoshima J, Sakagami H, Sakai Y, Sandri M, Sasakawa C, Sass M, Schneider C, Seglen PO, Seleverstov O, Settleman J, Shacka JJ, Shapiro IM, Sibirny A, Silva-Zacarin EC, Simon HU, Simone C, Simonsen A, Smith MA, Spanel-Borowski K, Srinivas V, Steeves M, Stenmark H, Stromhaug PE, Subauste CS, Sugimoto S, Sulzer D, Suzuki T, Swanson MS, Tabas I, Takeshita F, Talbot NJ, Talloczy Z, Tanaka K, Tanaka K, Tanida I, Taylor GS, Taylor JP, Terman A, Tettamanti G, Thompson CB, Thumm M, Tolkovsky AM, Tooze SA, Truant R, Tumanovska LV, Uchiyama Y, Ueno T, Uzcategui NL, van dK, I, Vaquero EC, Vellai T, Vogel MW, Wang HG, Webster P, Wiley JW, Xi Z, Xiao G, Yahalom J, Yang JM, Yap G, Yin XM, Yoshimori T, Yu L, Yue Z, Yuzaki M, Zabirnyk O, Zheng X, Zhu X and Deter RL. Guidelines for the

use and interpretation of assays for monitoring autophagy in higher eukaryotes. *Autophagy* 4: 151-175, 2008.

82. **Komatsu M, Waguri S, Koike M, Sou YS, Ueno T, Hara T, Mizushima N, Iwata J, Ezaki J, Murata S, Hamazaki J, Nishito Y, Iemura S, Natsume T, Yanagawa T, Uwayama J, Warabi E, Yoshida H, Ishii T, Kobayashi A, Yamamoto M, Yue Z, Uchiyama Y, Kominami E and Tanaka K**. Homeostatic levels of p62 control cytoplasmic inclusion body formation in autophagy-deficient mice. *Cell* 131: 1149-1163, 2007.

83. **Komatsu M, Waguri S, Ueno T, Iwata J, Murata S, Tanida I, Ezaki J, Mizushima N, Ohsumi Y, Uchiyama Y, Kominami E, Tanaka K and Chiba T**. Impairment of starvation-induced and constitutive autophagy in Atg7-deficient mice. *J Cell Biol* 169: 425-434, 2005.

84. **Kwiatkowski DJ and Manning BD**. Tuberous sclerosis: a GAP at the crossroads of multiple signaling pathways. *Hum Mol Genet* 14 Spec No. 2: R251-R258, 2005.

85. **Kwon J, Lee SR, Yang KS, Ahn Y, Kim YJ, Stadtman ER and Rhee SG**. Reversible oxidation and inactivation of the tumor suppressor PTEN in cells stimulated with peptide growth factors. *Proc Natl Acad Sci U S A* 101: 16419-16424, 2004.

86. **Lee JW, Park S, Takahashi Y and Wang HG**. The association of AMPK with ULK1 regulates autophagy. *PLoS One* 5: e15394, 2010.

87. **Leslie NR, Bennett D, Lindsay YE, Stewart H, Gray A and Downes CP**. Redox regulation of PI 3-kinase signalling via inactivation of PTEN. *EMBO J* 22: 5501-5510, 2003.

88. **Levine B and Klionsky DJ**. Development by self-digestion: molecular mechanisms and biological functions of autophagy. *Dev Cell* 6: 463-477, 2004.

89. **Levine S, Biswas C, Dierov J, Barsotti R, Shrager JB, Nguyen T, Sonnad S, Kucharchzuk JC, Kaiser LR, Singhal S and Budak MT**. Increased proteolysis, myosin depletion, and atrophic AKT-FOXO signaling in human diaphragm disuse. *Am J Respir Crit Care Med* 183: 483-490, 2011.

90. **Li L, Chen Y and Gibson SB**. Starvation-induced autophagy is regulated by mitochondrial reactive oxygen species leading to AMPK activation. *Cell Signal* 25: 50-65, 2013.

91. **Liang C, Feng P, Ku B, Dotan I, Canaani D, Oh BH and Jung JU**. Autophagic and tumour suppressor activity of a novel Beclin1-binding protein UVRAG. *Nat Cell Biol* 8: 688-699, 2006.

92. **Liang C, Lee JS, Inn KS, Gack MU, Li Q, Roberts EA, Vergne I, Deretic V, Feng P, Akazawa C and Jung JU**. Beclin1-binding UVRAG targets the class C Vps complex to coordinate autophagosome maturation and endocytic trafficking. *Nat Cell Biol* 10: 776-787, 2008.

93. **Liang HL, Sedlic F, Bosnjak Z and Nilakantan V**. SOD1 and MitoTEMPO partially prevent mitochondrial permeability transition pore opening, necrosis, and mitochondrial apoptosis after ATP depletion recovery. *Free Radic Biol Med* 49: 1550-1560, 2010.

94. **Liu ZP, Wang Z, Yanagisawa H and Olson EN**. Phenotypic modulation of smooth muscle cells through interaction of Foxo4 and myocardin. *Dev Cell* 9: 261-270, 2005.

95. **Lokireddy S, Wijesoma IW, Teng S, Bonala S, Gluckman PD, McFarlane C, Sharma M and Kambadur R**. The ubiquitin ligase Mul1 induces mitophagy in skeletal muscle in response to muscle-wasting stimuli. *Cell Metab* 16: 613-624, 2012.

96. **MacKenzie EL, Iwasaki K and Tsuji Y**. Intracellular iron transport and storage: from molecular mechanisms to health implications. *Antioxid Redox Signal* 10: 997-1030, 2008.

97. **Malicdan MC and Nishino I**. Autophagy in lysosomal myopathies. *Brain Pathol* 22: 82-88, 2012.

98. **Mammucari C, Milan G, Romanello V, Masiero E, Rudolf R, Del PP, Burden SJ, Di LR, Sandri C, Zhao J, Goldberg AL, Schiaffino S and Sandri M**. FoxO3 controls autophagy in skeletal muscle in vivo. *Cell Metab* 6: 458-471, 2007.

99. **Manning BD, Tee AR, Logsdon MN, Blenis J and Cantley LC**. Identification of the tuberous sclerosis complex-2 tumor suppressor gene product tuberin as a target of the phosphoinositide 3-kinase/akt pathway. *Mol Cell* 10: 151-162, 2002.

100. **Masiero E, Agatea L, Mammucari C, Blaauw B, Loro E, Komatsu M, Metzger D, Reggiani C, Schiaffino S and Sandri M**. Autophagy is required to maintain muscle mass. *Cell Metab* 10: 507-515, 2009.

101. **Masiero E and Sandri M**. Autophagy inhibition induces atrophy and myopathy in adult skeletal muscles. *Autophagy* 6: 307-309, 2010.

102. **Matsui Y, Kyoi S, Takagi H, Hsu CP, Hariharan N, Ago T, Vatner SF and Sadoshima J**. Molecular mechanisms and physiological significance of autophagy during myocardial ischemia and reperfusion. *Autophagy* 4: 409-415, 2008.

103. **Matsuzawa A and Ichijo H**. Stress-responsive protein kinases in redox-regulated apoptosis signaling. *Antioxid Redox Signal* 7: 472-481, 2005.

104. **McClung JM, Judge A, Talbert EE and Powers SK**. Calpain-1 is Required for Hydrogen Peroxide Induced Myotube Atrophy

1. *Am J Physiol Cell Physiol* 2008.

105. **Meijer AJ**. Amino acid regulation of autophagosome formation. *Methods Mol Biol* 445: 89-109, 2008.

106. **Mijaljica D, Prescott M and Devenish RJ**. Microautophagy in mammalian cells: revisiting a 40-year-old conundrum. *Autophagy* 7: 673-682, 2011.

107. **Miller JB, Teal SB and Stockdale FE**. Evolutionarily conserved sequences of striated muscle myosin heavy chain isoforms. Epitope mapping by cDNA expression. *J Biol Chem* 264: 13122-13130, 1989.

108. **Mizushima N, Sugita H, Yoshimori T and Ohsumi Y**. A new protein conjugation system in human. The counterpart of the yeast Apg12p conjugation system essential for autophagy. *J Biol Chem* 273: 33889-33892, 1998.

109. **Mizushima N, Yamamoto A, Matsui M, Yoshimori T and Ohsumi Y**. In vivo analysis of autophagy in response to nutrient starvation using transgenic mice expressing a fluorescent autophagosome marker. *Mol Biol Cell* 15: 1101-1111, 2004.

110. **Mizushima N, Yoshimori T and Ohsumi Y**. The role of Atg proteins in autophagosome formation. *Annu Rev Cell Dev Biol* 27: 107-132, 2011.

111. **Mofarrahi M, Sigala I, Guo Y, Godin R, Davis EC, Petrof B, Sandri M, Burelle Y and Hussain SN**. Autophagy and skeletal muscles in sepsis. *PLoS One* 7: e47265, 2012.

112. **Mofarrahi M, Guo Y, Haspel J, Choi AMK, Davis E, Gouspillou G, Hepple R, Godin R, Burelle Y and Hussain S**. Autophagic flux and oxidative capacity of skeletal muscles during acute starvation. *Autophagy* 9: 22-21, 2013.

113. **Mols M, Ceragioli M and Abee T**. Heat stress leads to superoxide formation in Bacillus cereus detected using the fluorescent probe MitoSOX. *Int J Food Microbiol* 151: 119-122, 2011.

114. **Murphy ME and Kehrer JP**. Oxidative stress and muscular dystrophy. *Chem Biol Interact* 69: 101-173, 1989.

115. **Nagpal P, Plant PJ, Correa J, Bain A, Takeda M, Kawabe H, Rotin D, Bain JR and Batt JA**. The ubiquitin ligase Nedd4-1 participates in denervation-induced skeletal muscle atrophy in mice. *PLoS ONE* 7: e46427, 2012.

116. **Narendra D, Tanaka A, Suen DF and Youle RJ**. Parkin is recruited selectively to impaired mitochondria and promotes their autophagy. *J Cell Biol* 183: 795-803, 2008.

117. **Nathan C**. Specificity of a third kind: reactive oxygen and nitrogen intermediates in cell signaling. *J Clin Invest* 111: 769-778, 2003.

118. **Nystrom GJ and Lang CH**. Sepsis and AMPK Activation by AICAR Differentially Regulate FoxO-1, -3 and -4 mRNA in Striated Muscle. *Int J Clin Exp Med* 1: 50-63, 2008.

119. **O'Leary MF, Vainshtein A, Carter HN, Zhang Y and Hood DA**. Denervation-induced mitochondrial dysfunction and autophagy in skeletal muscle of apoptosis-deficient animals. *Am J Physiol Cell Physiol* 303: C447-C454, 2012.

120. **Pallafacchina G, Calabria E, Serrano AL, Kalhovde JM and Schiaffino S**. A protein kinase B-dependent and rapamycin-sensitive pathway controls skeletal muscle growth but not fiber type specification. *Proc Natl Acad Sci U S A* 99: 9213-9218, 2002.

121. **Pattingre S, Tassa A, Qu X, Garuti R, Liang XH, Mizushima N, Packer M, Schneider MD and Levine B**. Bcl-2 antiapoptotic proteins inhibit Beclin 1-dependent autophagy. *Cell* 122: 927-939, 2005.

122. **Penna F, Costamagna D, Pin F, Camperi A, Fanzani A, Chiarpotto EM, Cavallini G, Bonelli G, Baccino FM and Costelli P**. Autophagic degradation contributes to muscle wasting in cancer cachexia. *Am j Pathol* 182: 1367-1378, 2013.

123. **Petiot A, Ogier-Denis E, Blommaart EF, Meijer AJ and Codogno P**. Distinct classes of phosphatidylinositol 3'-kinases are involved in signaling pathways that control macroautophagy in HT-29 cells. *J Biol Chem* 275: 992-998, 2000.

124. **Polge C, Heng AE, Jarzaguet M, Ventadour S, Claustre A, Combaret L, Bechet D, Matondo M, Uttenweiler-Joseph S, Monsarrat B, Attaix D and Taillandier D**. Muscle actin is polyubiquitinylated in vitro and in vivo and targeted for breakdown by the E3 ligase MuRF1. *FASEB J* 25: 3790-3802, 2011.

125. **Powers SK, Duarte J, Kavazis AN and Talbert EE**. Reactive oxygen species are signalling molecules for skeletal muscle adaptation. *Exp Physiol* 95: 1-9, 2010.

126. **Qiu J, Tsien C, Thapalaya S, Narayanan A, Weihl CC, Ching JK, Eghtesad B, Singh K, Fu X, Dubyak G, McDonald C, Almasan A, Hazen SL, Naga Prasad SV and Dasarathy S**. Hyperammonemia-mediated autophagy in skeletal muscle contributes to sarcopenia of cirrhosis. *Am J Physiol Endocrinol Metab* 303: E983-E993, 2012.

127. **Raben N, Hill V, Shea L, Takikita S, Baum R, Mizushima N, Ralston E and Plotz P**. Suppression of autophagy in skeletal muscle uncovers the accumulation of ubiquitinated proteins and their potential role in muscle damage in Pompe disease. *Hum Mol Genet* 17: 3897-3908, 2008.

128. **Ramachandran N, Munteanu I, Wang P, Aubourg P, Rilstone JJ, Israelian N, Naranian T, Paroutis P, Guo R, Ren ZP, Nishino I, Chabrol B, Pellissier JF, Minetti C, Udd B, Fardeau M, Tailor CS, Mahuran DJ, Kissel JT, Kalimo H, Levy N, Manolson MF, Ackerley CA and Minassian**

BA. VMA21 deficiency causes an autophagic myopathy by compromising V-ATPase activity and lysosomal acidification. *Cell* 137: 235-246, 2009.

129. **Reid MB**. Reactive oxygen and nitric oxide in skeletal muscle. *News Physiol Sci* 11: 114-119, 1996.

130. **Reid MB, Haack KE, Francik KM, Volberg PA, Kobzik L and Wes MS**. Reactive oxygen in skeletal muscle. I. Intracellular oxidant kinetics and fatigue *in vitro* . *J Appl Physiol* 73: 1797-1804, 1992.

131. **Reid MB, Khawli FA and Moody MR**. Reactive oxygen in skeletal muscle. III. Contractility of unfatigued muscle. *J Appl Physiol* 75: 1081-1087, 1993.

132. **Reid MB, Shoji T, Moody MR and Entman ML**. Reactive oxygen in skeletal muscle. II. Extracellular release of free radicals. *J Appl Physiol* 73: 1805-1809, 1992.

133. **Risson V, Mazelin L, Roceri M, Sanchez H, Moncollin V, Corneloup C, Richard-Bulteau H, Vignaud A, Baas D, Defour A, Freyssenet D, Tanti JF, Le-Marchand-Brustel Y, Ferrier B, Conjard-Duplany A, Romanino K, Bauche S, Hantai D, Mueller M, Kozma SC, Thomas G, Ruegg MA, Ferry A, Pende M, Bigard X, Koulmann N, Schaeffer L and Gangloff YG**. Muscle inactivation of mTOR causes metabolic and dystrophin defects leading to severe myopathy. *J Cell Biol* 187: 859-874, 2009.

134. **Robinson KA, Stewart CA, Pye QN, Nguyen X, Kenney L, Salzman S, Floyd RA and Hensley K**. Redox-sensitive protein phosphatase activity regulates the phosphorylation state of p38 protein kinase in primary astrocyte culture. *J Neurosci Res* 55: 724-732, 1999.

135. **Romanello V, Guadagnin E, Gomes L, Roder I, Sandri C, Petersen Y, Milan G, Masiero E, Del PP, Foretz M, Scorrano L, Rudolf R and Sandri M**. Mitochondrial fission and remodelling contributes to muscle atrophy. *EMBO J* 29: 1774-1785, 2010.

136. **Rusten TE, Vaccari T, Lindmo K, Rodahl LM, Nezis IP, Sem-Jacobsen C, Wendler F, Vincent JP, Brech A, Bilder D and Stenmark H**. ESCRTs and Fab1 regulate distinct steps of autophagy. *Curr Biol* 17: 1817-1825, 2007.

137. **Samuni A, Goldstein S, Russo A, Mitchell JB, Krishna MC and Neta P**. Kinetics and mechanism of hydroxyl radical and OH-adduct radical reactions with nitroxides and with their hydroxylamines. *J Am Chem Soc* 124: 8719-8724, 2002.

138. **Samuni A, Krishna CM, Riesz P, Finkelstein E and Russo A**. A novel metal-free low molecular weight superoxide dismutase mimic. *J Biol Chem* 263: 17921-17924, 1988.

139. **Sanchez AM, Candau RB, Csibi A, Pagano AF, Raibon A and Bernardi H**. The role of AMP-activated protein kinase in the coordination of skeletal muscle turnover and energy homeostasis. *Am J Physiol Cell Physiol* 303: C475-C485, 2012.

140. **Sanchez AM, Csibi A, Raibon A, Cornille K, Gay S, Bernardi H and Candau R**. AMPK promotes skeletal muscle autophagy through activation of forkhead FoxO3a and interaction with Ulk1. *J Cell Biochem* 113: 695-710, 2012.

141. **Sandri M**. Autophagy in skeletal muscle. *FEBS Lett* 584: 1411-1416, 2010.

142. **Sandri M**. Protein breakdown in muscle wasting: Role of autophagy-lysosome and ubiquitin-proteasome. *Int J Biochem Cell Biol* 2013.

143. **Sandri M, Sandri C, Gilbert A, Skurk C, Calabria E, Picard A, Walsh K, Schiaffino S, Lecker SH and Goldberg AL**. Foxo transcription factors induce the atrophy-related ubiquitin ligase atrogin-1 and cause skeletal muscle atrophy. *Cell* 117: 399-412, 2004.

144. **Sarbassov DD, Ali SM and Sabatini DM**. Growing roles for the mTOR pathway. *Curr Opin Cell Biol* 17: 596-603, 2005.

145. **Sarbassov DD, Guertin DA, Ali SM and Sabatini DM**. Phosphorylation and regulation of Akt/PKB by the rictor-mTOR complex. *Science* 307: 1098-1101, 2005.

146. **Sarbassov DD and Sabatini DM**. Redox regulation of the nutrient-sensitive raptor-mTOR pathway and complex. *J Biol Chem* 280: 39505-39509, 2005.

147. **Scherz-Shouval R and Elazar Z**. Regulation of autophagy by ROS: physiology and pathology. *trends biochem sci* 36: 30-38, 2011.

148. **Scherz-Shouval R, Shvets E, Fass E, Shorer H, Gil L and Elazar Z**. Reactive oxygen species are essential for autophagy and specifically regulate the activity of Atg4. *EMBO J* 26: 1749-1760, 2007.

149. **Schiaffino S and Reggiani C**. Fiber types in mammalian skeletal muscles. *Physiol Rev* 91: 1447-1531, 2011.

150. **Schweers RL, Zhang J, Randall MS, Loyd MR, Li W, Dorsey FC, Kundu M, Opferman JT, Cleveland JL, Miller JL and Ney PA**. NIX is required for programmed mitochondrial clearance during reticulocyte maturation. *Proc Natl Acad Sci U S A* 104: 19500-19505, 2007.

151. **Scott W, Stevens J and Binder-Macleod SA**. Human skeletal muscle fiber type classifications. *Phys Ther* 81: 1810-1816, 2001.

152. **Seo JH, Ahn Y, Lee SR, Yeol YC and Chung HK**. The major target of the endogenously generated reactive oxygen species in response to insulin stimulation is phosphatase and tensin homolog and not phosphoinositide-3 kinase (PI-3 kinase) in the PI-3 kinase/Akt pathway. *Mol Biol Cell* 16: 348-357, 2005.

153. **Shang L, Chen S, Du F, Li S, Zhao L and Wang X**. Nutrient starvation elicits an acute autophagic response mediated by Ulk1 dephosphorylation and its subsequent dissociation from AMPK. *Proc Natl Acad Sci U S A* 108: 4788-4793, 2011.

154. **Shi Y, Yan H, Frost P, Gera J and Lichtenstein A**. Mammalian target of rapamycin inhibitors activate the AKT kinase in multiple myeloma cells by up-regulating the insulin-like growth factor receptor/insulin receptor substrate-1/phosphatidylinositol 3-kinase cascade. *Mol Cancer Ther* 4: 1533-1540, 2005.

155. **Shigemitsu K, Tsujishita Y, Hara K, Nanahoshi M, Avruch J and Yonezawa K**. Regulation of translational effectors by amino acid and mammalian target of rapamycin signaling pathways. Possible involvement of autophagy in cultured hepatoma cells. *J Biol Chem* 274: 1058-1065, 1999.

156. **Smith IJ, Lecker SH and Hasselgren PO**. Calpain activity and muscle wasting in sepsis. *Am J Physiol Endocrinol Metab* 295: E762-E771, 2008.

157. **Smuder AJ, Kavazis AN, Min K and Powers SK**. Exercise protects against doxorubicin-induced oxidative stress and proteolysis in skeletal muscle. *J Appl Physiol* 110: 935-942, 2011.

158. **Solomon V, Baracos V, Sarraf P and Goldberg AL**. Rates of ubiquitin conjugation increase when muscles atrophy, largely through activation of the N-end rule pathway. *Proc Natl Acad Sci U S A* 95: 12602-12607, 1998.

159. **Sorimachi H, Imajoh-Ohmi S, Emori Y, Kawasaki H, Ohno S, Minami Y and Suzuki K**. Molecular cloning of a novel mammalian calcium-dependent protease distinct from both m- and mu-types. Specific expression of the mRNA in skeletal muscle. *J Biol Chem* 264: 20106-20111, 1989.

160. **Southgate RJ, Neill B, Prelovsek O, El-Osta A, Kamei Y, Miura S, Ezaki O, McLoughlin TJ, Zhang W, Unterman TG and Febbraio MA**. FOXO1 regulates the expression of 4E-BP1 and inhibits mTOR signaling in mammalian skeletal muscle. *J Biol Chem* 282: 21176-21186, 2007.

161. **St-Pierre J, Buckingham JA, Roebuck SJ and Brand MD**. Topology of superoxide production from different sites in the mitochondrial electron transport chain. *J Biol Chem* 277: 44784-44790, 2002.

162. **Sundaram P, Pang Z, Miao M, Yu L and Wing SS**. USP19-deubiquitinating enzyme regulates levels of major myofibrillar proteins in L6 muscle cells. *Am J Physiol Endocrinol Metab* 297: E1283-E1290, 2009.

163. **Taillandier D, Aurousseau E, Meynial-Denis D, Bechet D, Ferrara M, Cottin P, Ducastaing A, Bigard X, Guezennec CY, Schmid HP and .** Coordinate activation of lysosomal, Ca 2+-activated and ATP-ubiquitin-dependent proteinases in the unweighted rat soleus muscle. *Biochem J* 316 (Pt 1): 65-72, 1996.

164. **Tidball JG**. Inflammatory processes in muscle injury and repair. *Am J Physiol Regul Integr Comp Physiol* 288: R345-R353, 2005.

165. **Tidball JG and Spencer MJ**. Expression of a calpastatin transgene slows muscle wasting and obviates changes in myosin isoform expression during murine muscle disuse. *J Physiol* 545: 819-828, 2002.

166. **Tintignac LA, Lagirand J, Batonnet S, Sirri V, Leibovitch MP and Leibovitch SA**. Degradation of MyoD mediated by the SCF (MAFbx) ubiquitin ligase. *J Biol Chem* 280: 2847-2856, 2005.

167. **Tran H, Brunet A, Griffith EC and Greenberg ME**. The many forks in FOXO's road. *Sci STKE* 2003: RE5, 2003.

168. **Underwood BR, Imarisio S, Fleming A, Rose C, Krishna G, Heard P, Quick M, Korolchuk VI, Renna M, Sarkar S, Garcia-Arencibia M, O'Kane CJ, Murphy MP and Rubinsztein DC**. Antioxidants can inhibit basal autophagy and enhance neurodegeneration in models of polyglutamine disease. *Hum Mol Genet* 19: 3413-3429, 2010.

169. **Veal EA, Day AM and Morgan BA**. Hydrogen peroxide sensing and signaling. *Mol Cell* 26: 1-14, 2007.

170. **Vergne I, Roberts E, Elmaoued RA, Tosch V, Delgado MA, Proikas-Cezanne T, Laporte J and Deretic V**. Control of autophagy initiation by phosphoinositide 3-phosphatase Jumpy. *EMBO J* 28: 2244-2258, 2009.

171. **Wang RC, Wei Y, An Z, Zou Z, Xiao G, Bhagat G, White M, Reichelt J and Levine B**. Akt-mediated regulation of autophagy and tumorigenesis through Beclin 1 phosphorylation. *Science* 338: 956-959, 2012.

172. **Wang X, Blagden C, Fan J, Nowak SJ, Taniuchi I, Littman DR and Burden SJ**. Runx1 prevents wasting, myofibrillar disorganization, and autophagy of skeletal muscle. *Genes Dev* 19: 1715-1722, 2005.

173. **Wani R, Qian J, Yin L, Bechtold E, King SB, Poole LB, Paek E, Tsang AW and Furdui CM**. Isoform-specific regulation of Akt by PDGF-induced reactive oxygen species. *Proc Natl Acad Sci U S A* 108: 10550-10555, 2011.

174. **Wenz T, Rossi SG, Rotundo RL, Spiegelman BM and Moraes CT**. Increased muscle PGC-1alpha expression protects from sarcopenia and metabolic disease during aging. *Proc Natl Acad Sci U S A* 106: 20405-20410, 2009.

175. **Westerblad H, Bruton JD and Katz A**. Skeletal muscle: energy metabolism, fiber types, fatigue and adaptability. *Exp Cell Res* 316: 3093-3099, 2010.

176. **Winterbourn CC**. Reconciling the chemistry and biology of reactive oxygen species. *Nat Chem Biol* 4: 278-286, 2008.

177. **Wohlgemuth SE, Seo AY, Marzetti E, Lees HA and Leeuwenburgh C**. Skeletal muscle autophagy and apoptosis during aging: effects of calorie restriction and life-long exercise. *Exp Gerontol* 45: 138-148, 2010.

178. **Xanthoudakis S, Miao GG and Curran T**. The redox and DNA-repair activities of Ref-1 are encoded by nonoverlapping domains. *Proc Natl Acad Sci U S A* 91: 23-27, 1994.

179. **Yamamoto A, Tagawa Y, Yoshimori T, Moriyama Y, Masaki R and Tashiro Y**. Bafilomycin A1 prevents maturation of autophagic vacuoles by inhibiting fusion between autophagosomes and lysosomes in rat hepatoma cell line, H-4-II-E cells. *Cell Struct Funct* 23: 33-42, 1998.

180. **Yang Q and Guan KL**. Expanding mTOR signaling. *Cell Res* 17: 666-681, 2007.

181. **Youle RJ and Narendra DP**. Mechanisms of mitophagy. *Nat Rev Mol Cell Biol* 12: 9-14, 2011.

182. **Yu ZQ, Ni T, Hong B, Wang HY, Jiang FJ, Zou S, Chen Y, Zheng XL, Klionsky DJ, Liang Y and Xie Z**. Dual roles of Atg8-PE deconjugation by Atg4 in autophagy. *Autophagy* 8: 883-892, 2012.

183. **Zhang H, Bosch-Marce M, Shimoda LA, Tan YS, Baek JH, Wesley JB, Gonzalez FJ and Semenza GL**. Mitochondrial autophagy is an HIF-1-dependent adaptive metabolic response to hypoxia. *J Biol Chem* 283: 10892-10903, 2008.

184. **Zhang J and Ney PA**. Role of BNIP3 and NIX in cell death, autophagy, and mitophagy. *Cell Death Differ* 16: 939-946, 2009.

185. **Zhao J, Brault JJ, Schild A, Cao P, Sandri M, Schiaffino S, Lecker SH and Goldberg AL**. FoxO3 coordinately activates protein degradation by the autophagic/lysosomal and proteasomal pathways in atrophying muscle cells. *Cell Metab* 6: 472-483, 2007.

186. **Zhao J, Brault JJ, Schild A and Goldberg AL**. Coordinate activation of autophagy and the proteasome pathway by FoxO transcription factor. *Autophagy* 4: 378-380, 2008.

187. **Zhao K, Zhao GM, Wu D, Soong Y, Birk AV, Schiller PW and Szeto HH**. Cell-permeable peptide antioxidants targeted to inner mitochondrial membrane inhibit mitochondrial swelling, oxidative cell death, and reperfusion injury. *J Biol Chem* 279: 34682-34690, 2004.